

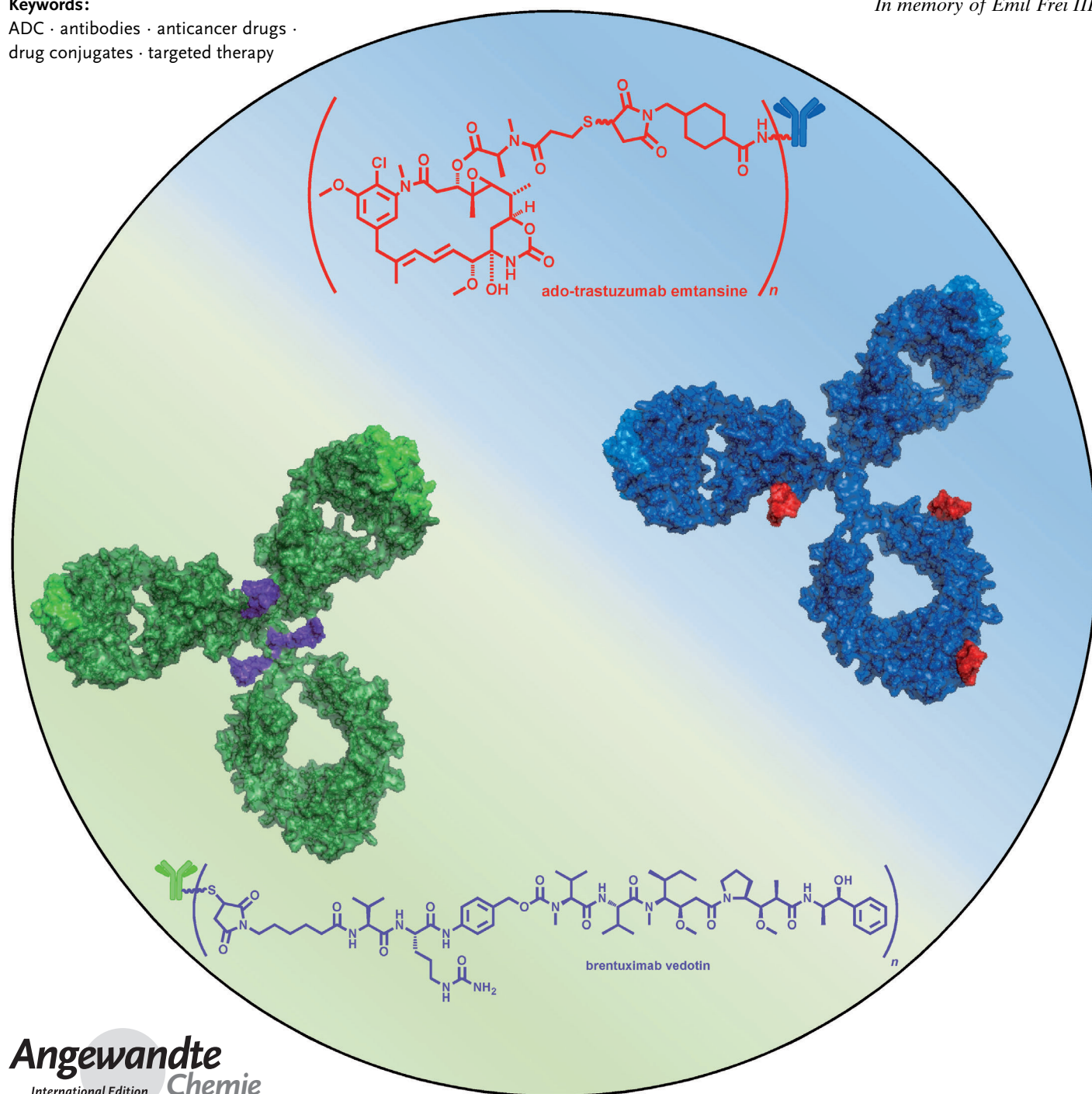
# Antibody–Drug Conjugates: An Emerging Concept in Cancer Therapy

Ravi V. J. Chari,\* Michael L. Miller, and Wayne C. Widdison

**Keywords:**

ADC · antibodies · anticancer drugs · drug conjugates · targeted therapy

*In memory of Emil Frei III*



**T**raditional cancer chemotherapy is often accompanied by systemic toxicity to the patient. Monoclonal antibodies against antigens on cancer cells offer an alternative tumor-selective treatment approach. However, most monoclonal antibodies are not sufficiently potent to be therapeutically active on their own. Antibody–drug conjugates (ADCs) use antibodies to deliver a potent cytotoxic compound selectively to tumor cells, thus improving the therapeutic index of chemotherapeutic agents. The recent approval of two ADCs, brentuximab vedotin and ado-trastuzumab emtansine, for cancer treatment has spurred tremendous research interest in this field. This Review touches upon the early efforts in the field, and describes how the lessons learned from the first-generation ADCs have led to improvements in every aspect of this technology, i.e., the antibody, the cytotoxic compound, and the linker connecting them, leading to the current successes. The design of ADCs currently in clinical development, and results from mechanistic studies and preclinical and clinical evaluation are discussed. Emerging technologies that seek to further advance this exciting area of research are also discussed.

## 1. Introduction

For the better part of the twentieth century, chemotherapy, or “treatment with chemicals” was the predominant modality for cancer treatment.<sup>[1,2]</sup> The use of chemotherapeutic agents for the treatment of cancer is based on the premise that these agents would preferentially kill rapidly dividing cancer cells, while sparing normal cells. The first class of chemotherapeutic agents to be tested in humans were the nitrogen mustards, chlorambucil and cyclophosphamide, which exert cellular cytotoxicity by alkylation of DNA. Although success was short lived, the initial promise spurred the development of a steady stream of new anticancer agents with improved activity. The recognition that folic acid stimulates cancer cell growth led to the synthesis of antifolates, such as methotrexate, as antitumor agents. The elucidation of the structure of DNA led to compounds that interfered with DNA synthesis and caused cell death. These included nucleoside analogues, such as thioguanine, 5-fluorouracil, and cytosine arabinoside (ara-C). Subsequently, DNA-interacting agents, such as cisplatin, and antitumor antibiotics derived from bacterial fermentation, such as actinomycin D and the anthracyclines entered the foray of drugs to treat cancer. Chemotherapeutic agents targeting tubulin (e.g. the *Vinca* alkaloids from plants) also entered clinical evaluation.

Although by the late 1980s, there was a plethora of drugs in the anticancer armamentarium, their effectiveness continued to be plagued by the lack of tumor selectivity, resulting in the killing of proliferating normal cells, such as those of the bone marrow and gastrointestinal tract. Most anticancer drugs had to be used near their maximum tolerated dose (MTD) to achieve a clinically meaningful therapeutic effect. A significant milestone in cancer chemotherapy was the introduction of the concept of drug combinations.<sup>[3]</sup> It was realized that cancer drugs with non-overlapping toxicity

profiles and different mechanisms of action could often be combined at full doses with resultant additive or synergistic effect and improved antitumor activity. Thus, multidrug therapy became a standard modality for the treatment of most cancers. With such intensive chemotherapy, systemic toxicity to the host remains a major drawback of cytotoxic drugs in cancer, and cures are achieved only in a small set of cancers.

The limited clinical efficacy of anticancer drugs, whether used alone or in combination, could be attributed to the insufficient therapeutic window of these compounds, that is, the inability to kill a sufficient number of cancer cells without causing toxicity. For example, it has been estimated that more than 99 % of the cells in the tumor have to be killed to achieve a complete remission in the patient, with significantly greater degree of cell kill required to achieve tumor eradication.<sup>[3]</sup> In order to improve the therapeutic index of cancer drugs, either the potency of the cytotoxic agent had to be improved to lower the minimum effective dose (MED), or the tumor selectivity improved to increase the maximum tolerated dose (Figure 1). An ideal solution would be the development of agents that would both decrease the MED and increase the MTD, thus increasing the overall therapeutic index of the cancer drug.

The recognition that many anticancer drugs were derived from natural sources, such as plants and marine or microbial organisms, stimulated active research in the area of natural

## From the Contents

1. Introduction	3797
2. Targeted Therapies	3799
3. First-Generation Antibody–Drug Conjugates	3801
4. Improved Antibody–Drug Conjugates: Key Requirements	3802
5. Antimitotic Agents as ADC Payloads	3803
6. DNA Agents as ADC Payloads	3813
7. Clinical Results	3818
8. Emerging Technologies	3819
9. Summary and Outlook	3823

[\*] Dr. R. V. J. Chari, Dr. M. L. Miller, Dr. W. C. Widdison  
ImmunoGen, Inc.  
830 Winter St, Waltham, MA 02451 (USA)  
E-mail: ravi.chari@immunogen.com  
Homepage: <http://www.immunogen.com>

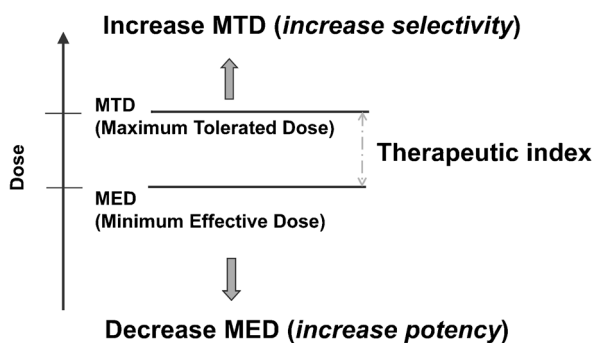


Figure 1. Approach to optimize the therapeutic index.

products by medicinal chemists seeking to discover new cytotoxic compounds with much higher potency than the known anticancer drugs. One of the first such compounds that garnered a lot of excitement was maytansine (**1**), a macrocyclic molecule belonging to the family of compounds termed maytansinoids, which were isolated from the Ethiopian shrub *Maytenus ovatus* by Kupchan et al.<sup>[4,5]</sup> Maytansine was found to be a strong inhibitor of tubulin polymerization, and thus a highly potent mitotic inhibitor.<sup>[6]</sup> It was one of the first compounds to kill cancer cells with  $IC_{50}$  values in the picomolar range, and thus was several orders of magnitude more cytotoxic than clinically used anticancer agents, such as doxorubicin, methotrexate, and 5-fluorouracil. Maytansine was rapidly advanced into human clinical evaluation. However, after Phase II clinical studies, the development of maytansine was discontinued because of insufficient antitumor activity. Consistent with its high in vitro potency, the MTD achieved in humans ( $2 \text{ mg m}^{-2}$ ) was much lower than that of anticancer drugs, such as doxorubicin (dose  $60\text{--}75 \text{ mg m}^{-2}$ ).<sup>[7]</sup> The main dose-limiting toxicities associated with maytansine treatment were effects on the gastrointestinal tract and peripheral neuropathy.

Subsequently, a few other potent tubulin-interacting agents were discovered and advanced to clinical evaluation (Figure 2). Pettit and co-workers isolated a family of cytotoxic peptides, termed the dolastatins, from the marine shell-less mollusk *Dolabella auricularia*. The most studied members of this family are the linear peptides dolastatin 10 (**2a**) and dolastatin 15 (**2b**).<sup>[8,9]</sup> Like maytansine, these compounds are also potent inhibitors of tubulin polymerization and induced cancer cell death in vitro at picomolar concentrations. In Phase I clinical studies, the MTD of **2a** was found to be

$0.4 \text{ mg m}^{-2}$ , which was even lower than that of maytansine.<sup>[10]</sup> Dose-limiting toxicities were mainly of haematologic nature and included neutropenia and granulocytopenia. Phase II clinical trials in a number of cancer indications, including melanoma, renal cancer, sarcomas, and breast cancer, failed to demonstrate clinical benefit, and the development of dolastatin 10 was discontinued.<sup>[11]</sup> The dolastatin 15 analogue cemadotin (**2c**) and the next-generation analogue tasidotin (**2d**), which was designed to be metabolically stable through its resistance to hydrolysis by prolyl oligopeptidases, were also evaluated in human clinical trials and failed to demonstrate meaningful activity. The lack of therapeutic benefit of these compounds did not deter the development of another class of potent tubulin agents, the cryptophycins, a family of macrocyclics found in the blue-green alga *Nostoc* sp. (cyanobacteria). Cryptophycin 1 (**3a**) was the main component of the algal extract and was responsible for most of the cytotoxic activity. The synthetic analogue cryptophycin 52 (**3b**), which bears a gem-dimethyl substituent at C6 of the C subunit, was found to kill cancer cells in vitro at picomolar concentrations, and was advanced to clinical evaluation.<sup>[12]</sup> However, the dose achieved was very low (MTD of  $1.5 \text{ mg m}^{-2}$ ) and sufficient therapeutic activity was not attained.<sup>[13]</sup> Thus, the cryptophycins joined the ranks of the other highly potent tubulin agents that failed to live up to the promise that higher potency would translate to improved clinical activity. One exception to this trend is the recent approval of eribulin mesylate (**3c**) for the treatment of metastatic breast cancer. This drug is a fully synthetic analogue of halichondrin, a tubulin polymerization inhibitor derived from the marine sponge *Halichondria okadai*.<sup>[14]</sup>

While clinical success with these cytotoxic agents was elusive, it was not clear whether the lack of therapeutic activity was due to the extremely high potency of these drugs, leading to toxicity at low doses, or their mechanism of action, with all of them being inhibitors of tubulin polymerization. Results from clinical testing of potent drugs (Figure 3) with an alternative mechanism of cell killing could provide some insight. The isolation and structure elucidation of the microbial natural product CC-1065 (**4a**), a highly cytotoxic, sequence-selective DNA-minor-groove binder and DNA-alkylating agent, initiated the synthesis of a panel of simpler analogues.<sup>[15]</sup> These compounds retained the picomolar in vitro potency of the parent compound toward cancer cells. Several of these compounds, including adozelesin (**4b**), a prodrug form carzelesin (**4c**), an even more potent dimeric



Ravi V. J. Chari received his Ph.D. degree in Chemistry from the University of Detroit. He then pursued postdoctoral work at the School of Medicine of Yale University. Subsequently, he joined the Dana-Farber Cancer Institute/Harvard Medical School as a research scientist. In 1988, he joined ImmunoGen where he began research on antibody–drug conjugates for cancer. He is currently Executive Director, Chemistry & Biochemistry.



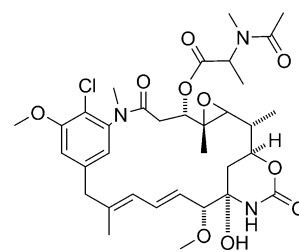
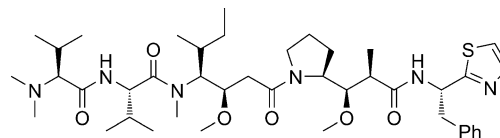
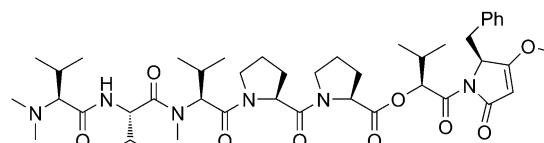
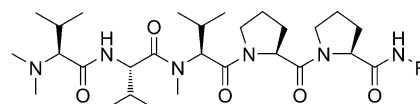
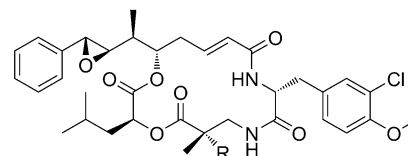
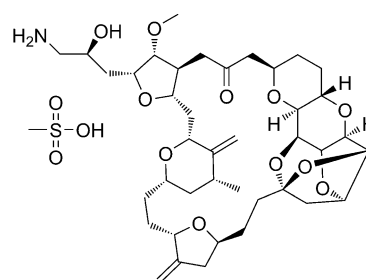
Michael L. Miller received his B.S. in 1994 from Memphis State University and his Ph.D. in 1998 at the University of Memphis. He pursued his postdoctoral research with Professor Iwao Ojima at the State University of New York at Stony Brook. In 2000, he joined the Chemistry Department at ImmunoGen, Inc., focusing his efforts on the development of potent compounds for use in antibody–drug conjugates.

compound bizelesin (**4d**), and the synthetic duocarmycin analogue KW-2189 (**4e**), were evaluated in human clinical trials.<sup>[16–19]</sup> These DNA-alkylating agents suffered the same fate as the potent tubulin agents described above, with very low clinically achievable doses (ranging from 0.001 mgm<sup>−2</sup> for **4d** to 0.4 mgm<sup>−2</sup> for **4e**) and insufficient activity. Recently, the pyrrolobenzodiazepine dimer SJG-136 (**4f**), a highly cytotoxic DNA crosslinker, has completed Phase I clinical evaluation, and again a low MTD (0.045 mgm<sup>−2</sup>) was achieved.<sup>[20]</sup> This drug is currently undergoing Phase II clinical evaluation. Thus, with few exceptions, merely increasing the cell-killing power of cytotoxic drugs does not appear to increase the therapeutic index of chemotherapy.

## 2. Targeted Therapies

Targeted therapy approaches seek to specifically interfere with molecular targets and pathways that are important for the proliferation of cancer cells. These targets are preferentially expressed either intracellularly or on the surface of tumor cells. Thus, targeted therapy offers the potential to generate agents that will be selectively cytotoxic to tumor cells, coupled with lower toxicity to the host, resulting in a larger therapeutic index. The major areas of focus include a) inhibitors of receptor tyrosine kinases, b) monoclonal antibodies, c) antibody–drug conjugates (ADCs), d) small targeting molecule–drug conjugates, and e) antisense and siRNA approaches. The initial clinical success of the targeted therapy approach has led to a burgeoning effort in these areas of cancer drug development. In the one-year period from October 2011 to October 2012, four of the seven cancer drugs approved by the FDA are targeted agents, further validating the promise of this approach.

One of the most popular targets for medicinal chemists in the field of cancer research are tyrosine kinases, enzymes that catalyze the transfer of the terminal phosphate group from adenosine triphosphate to the target protein. In cancer cells, some key tyrosine kinases are not properly regulated resulting in excessive phosphorylation of target proteins causing sustained signal transduction and cell proliferation. Additionally, tyrosine kinase may be over-expressed in tumor cells or exist in an aberrant (mutant) form that stimulates cancer cell growth.<sup>[21,22]</sup> A majority of these kinase inhibitors are heterocyclic compounds that compete with ATP for binding to the active conformational form of the enzyme. Imatinib


Maytansine (**1**)

Dolastatin 10 (**2a**)

Dolastatin 15 (**2b**)

Cemadotin (R = Bn) (**2c**)  
Tasidotin (R = tBu) (**2d**)

Cryptophycin 1 (R = H) (**3a**)  
Cryptophycin 52 (R = Me) (**3b**)

Eribulin mesylate (**3c**)

**Figure 2.** Structures of tubulin-binding cytotoxic agents.

mesylate was the first compound in this class to be approved by the FDA in 2001 for the treatment of chronic myelogenous leukemia (CML). Imatinib was designed to target the BCR-ABL protein, a mutant fusion protein that is present in leukemic cells in almost all CML patients. Imatinib competitively inhibits the binding of ATP to the BCR-ABL tyrosine kinase and specifically inhibits the proliferation of CML cells.



Wayne C. Widdison received his Ph.D. degree in Organic Chemistry with Professor John E. Baldwin at Syracuse University in 1991. He then pursued postdoctoral work at Stanford University. He joined the chemistry department at ImmunoGen in 1993, where he is currently a Principal Scientist. His research is focused on the development of maytansinoids and linkers for the preparation of antibody–drug conjugates.



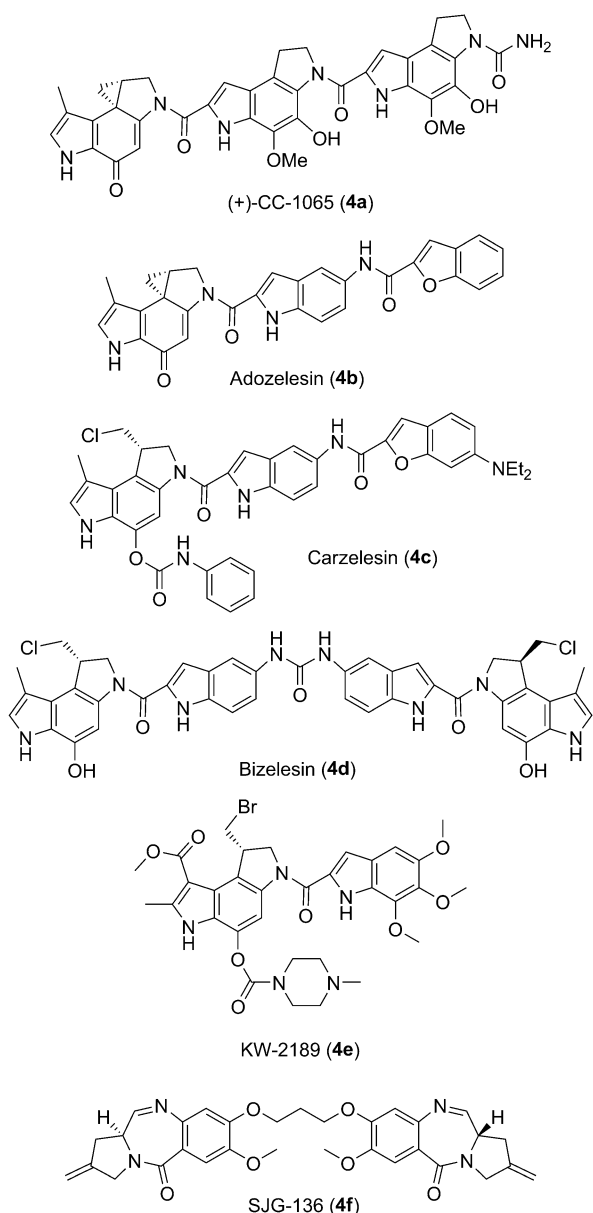


**Figure 3.** Structures of DNA-alkylating/cross-linking cytotoxic agents.

Success with imatinib was followed two years later with the approval of gefitinib, a selective inhibitor of the epidermal growth factor receptor tyrosine kinase. Thus far, at least 20 kinase inhibitors targeting different tumor indications have been approved. Many of the early kinase inhibitors exert their cytotoxic effect by targeting a specific kinase. In order to increase the treatment population, inhibitors that hit more than one target (multitargeted) are actively being pursued. It is not yet clear whether the lower selectivity of these types of agents would lead to greater adverse effects.

Another emerging targeted therapy approach is the use of small molecules that selectively bind to the surface of tumor cells to deliver a cytotoxic compound.<sup>[23]</sup> The most advanced compound in this class is a folate–Vinca alkaloid conjugate. In this conjugate, the tumor-targeting element, folic acid, binds with high affinity to the folate receptor that is over-expressed

on the surface of a number of tumors, notably ovarian and non-small-cell lung cancers. The construct consists of folic acid linked through a disulfide bond to desacetylvinblastine monohydrazide with a pentapeptide spacer. The folate conjugate showed good dose-dependent antitumor activity in a folate-receptor-positive tumor xenograft model, and was significantly more active than the unconjugated Vinca drug. Co-administration of an excess of unconjugated folic acid abrogated the antitumor activity of the conjugate, demonstrating tumor specificity.<sup>[24,25]</sup> This conjugate is currently in advanced clinical trials.

## 2.1. Monoclonal Antibodies in Cancer

The recognition that cancer cells possess specific molecular markers that play a role in tumor growth or progression has opened the door to specifically target these markers. These markers, also known as antigens, are typically cell-surface proteins, glycoproteins, or carbohydrates. Ideally, they are selectively expressed on the surface of tumor cells with minimal expression in normal human tissues. In many cases, the antigen may be overexpressed or present in mutated form on cancer cells. Immunization of mice with human cancer cells or purified antigens elicits a target-specific antibody response in the sera of these animals. While these antibodies could specifically bind to the target antigen, they are often obtained in low yield and as a mixture containing antibodies to nonspecific targets. The advent of the hybridoma technology pioneered by Kohler and Milstein in 1975<sup>[26]</sup> represented a significant advancement enabling production of large amounts of a single purified antibody to the antigen of interest. In this technique, antibody-producing B lymphocytes are isolated from the mice and immortalized by fusion with a mouse myeloma cell line. The resulting clonal cells, also known as hybridomas, can be cultured *in vitro* in tissue culture flasks or bioreactors to produce the specific monoclonal antibody (mAb). The efficiency of tumor cell kill by monoclonal antibodies can range widely, from poor to high depending on the nature of the target antigen. Antibodies can induce cancer cell death by a multitude of mechanisms, including a) immune-mediated functions, such as antibody-dependent cellular cytotoxicity (ADCC), b) complement-dependent cytotoxicity (CDC), c) antibody-dependent phagocytosis, d) interference with tumor-cell signaling pathways, often achieved through receptor blockage, e) depletion of circulating tumor cells by direct binding to the antibody, f) apoptosis, and g) immune modulation of T-cell function.<sup>[27,28]</sup>

The first human clinical trial with a monoclonal antibody was conducted in 1980 when a lymphoma patient was treated with the murine monoclonal antibody AB 89.<sup>[29]</sup> In the ensuing years, clinical trials with a number of murine monoclonal antibodies were conducted. An emerging theme from these trials was the development of an immune response to the murine monoclonal antibody, a foreign protein, with the generation of human anti-mouse antibodies (HAMA), resulting in rapid clearance of the murine antibody from circulation. Advances in recombinant DNA technology have

enabled the generation of engineered antibodies in which protein sequences of the murine antibody are replaced by sequences naturally occurring in human antibodies, without affecting the specific binding of the antibody to its target antigen. In the first of these constructs, molecular biologists merely replaced the entire constant regions of the murine antibody with the corresponding human constant region sequences, while retaining the murine variable domains (Fv) responsible for antigen binding (Figure 4). These “chimeric”

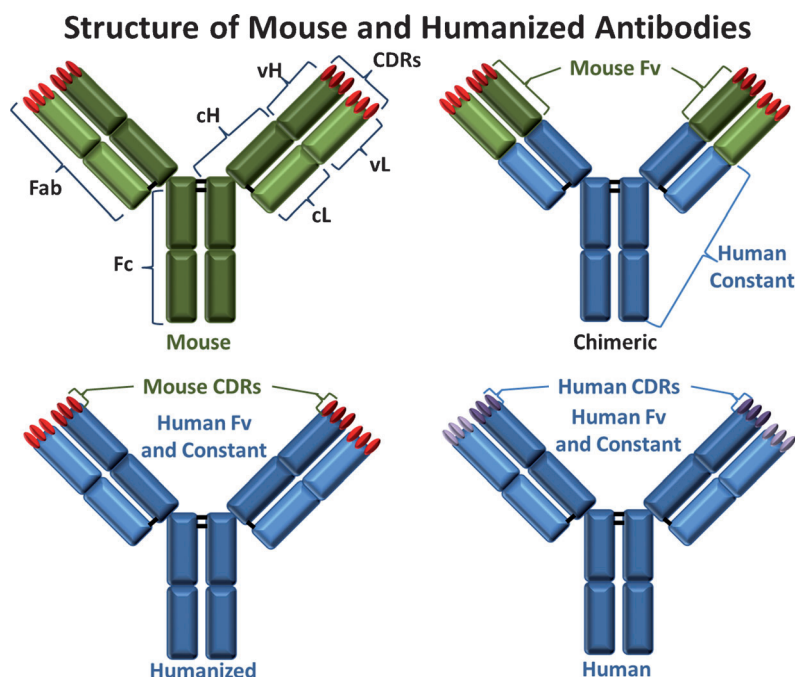


**Figure 4.** A cartoon representation of mouse (green), chimeric, humanized, and human (blue) antibodies. The antibody subdomains are marked, including Fab, Fc, heavy-chain variable (vH), light-chain variable (vL), heavy-chain constant (cH), light-chain constant (cL), and the complementarity determining regions (CDRs).

antibodies still contained a significant number of murine residues, so further antibody engineering advancements led to new “humanization” methods that facilitated the replacement of murine Fv sequences with the human antibody Fv sequences. In the humanized antibody, only the essential antigen recognition murine residues encompassing the complementarity determining regions (CDRs) within the Fv domains are preserved, while the remainder of the murine Fv is replaced with human Fv sequences. The advent of phage display technology and transgenic mice bearing the human repertoire introduced new avenues for generating fully human antibodies requiring no additional engineering for human therapeutic development.<sup>[30]</sup> With these advances, it has been possible to reduce or eliminate the immune response previously noted with murine antibodies. In addition, the circulation half-life of these new constructs is significantly longer ( $T_{1/2}$  up to three weeks) than that of their murine counterparts (typically two to three days).

The first monoclonal antibody for the treatment of cancer, rituximab, was approved by the U.S. FDA in 1997 for use in patients with relapsed or refractory, CD-20 positive, B-cell, low-grade or follicular non-Hodgkin’s lymphoma.<sup>[31]</sup> Rituximab is a chimeric antibody that binds to the CD20 antigen expressed on the surface of a majority of B-cell lymphomas. Subsequently, the anti-CD52 antibody alemtuzumab, and the anti-CD20 antibody ofatumumab were approved for the treatment of chronic lymphocytic leukemia. While the three

approved antibodies for hematologic malignancies are used as single agents, the FDA-approved antibodies for solid tumors often display only modest antitumor activity and are typically used together with chemotherapeutic agents. Thus, the humanized antibodies trastuzumab and pertuzumab targeting the HER-2 antigen, which is over-expressed on a subset of breast cancers and also some gastric tumors, are often used with chemotherapy. Similarly, the anti-EGF receptor antibodies cetuximab and panitumumab are used in combination with chemotherapy for the treatment of colorectal and head and neck cancers. Bevacizumab, an anti-angiogenic antibody that binds to vascular endothelial growth factor A, has been approved for treatment in combination with chemotherapy in a number of solid tumor indications. Such combination therapy has the drawback of preserving the toxic side effects of the cytotoxic drug. Recently, ipilimumab, an antibody that activates the immune system by targeting CTLA-4, has been approved for the treatment of patients with late-stage melanoma. Ipilimumab represents one of the few antibodies with sufficient activity to be used as a single agent in the treatment of solid tumors. In the 32 years since the first monoclonal antibody was evaluated in the clinic, only eight have been approved thus far for the treatment of cancer, and only two cell-surface targets, two members

of the ErbB receptor family (HER2 and EGFR), have been successfully targeted by antibodies for treating solid tumors.

### 3. First-Generation Antibody–Drug Conjugates

The concept of antibody–drug conjugates (ADCs) first evolved from the need to improve the tumor selectivity of clinically used anticancer drugs. While the role of monoclonal antibodies in cancer was still being defined, it was clear that many antibodies displayed preferential binding to tumor cells and could serve as a vehicle for selective delivery of the anticancer drug to the tumor. Thus, in the first set of ADCs to be prepared and tested, the anticancer drugs methotrexate, vinblastine, doxorubicin, and melphalan were linked to monoclonal antibodies. It was recognized early on, that the nature of the linker connecting the monoclonal antibody and drug was important. Once internalized into a target cell, some intracellular release mechanism should cleave the linker to

release the active drug. Among the utilized linkers were acid-labile linkers that relied on the acidic pH value ( $\approx 5$ ) of the intracellular compartment, the endosome, and enzyme-labile linkers that relied on lysosomal enzymes, such as peptidases and esterases, for cleavage.

In vitro evaluation of these first-generation conjugates on target tumor cell lines showed that, in most cases, these conjugates were only moderately potent and often less active than the parent drug. Target-selective potency was rarely demonstrated in vitro, suggesting that the choice of linkers in these conjugates was not appropriate. Nevertheless, researchers pursued the evaluation of antitumor activity of these conjugates in human xenograft models in mice. Significant localization of an antibody–methotrexate conjugate at the tumor was demonstrated. Within 3 h after administration, as much as 15% of the injected dose of conjugate had accumulated per gram of tumor.<sup>[32]</sup> Researchers were eager to see whether the impressive tumor localization would lead to significant antitumor activity in vivo. The in vivo antitumor activity of vinblastine and doxorubicin, linked to antibodies through acid-labile bonds, was shown to be superior to that of the corresponding unconjugated drugs.<sup>[33,34]</sup>

These encouraging preclinical results led to the clinical evaluation of four candidates (Figure 5). A conjugate of the murine KS1/4 antibody with the cytotoxic drug methotrexate (**6a**), linked through an amide bond, was evaluated in two Phase I clinical trials in patients with NSCLC.<sup>[35]</sup> Immunohistochemical (IHC) staining of carcinoma biopsies of the patients (post-treatment) provided convincing evidence of tumor localization of the conjugate. However, little evidence of therapeutic benefit or clinical response was observed in either study. Since the antibody that was used was of murine origin, the conjugate elicited an immune response in a majority of patients with HAMA observed in circulation within three weeks of treatment. The development of a HAMA response posed the risk of faster clearance of the ADC from circulation during repeat dosing. The murine KS1/4 antibody was also linked to desacetylvinblastine, through an esterase-labile hemisuccinate link (KS1/4-DAVLB, **6b**) or an acid-labile hydrazone bond (KS1/4-DAVLBH, **6c**). Both constructs were evaluated in human clinical trials.<sup>[36,37]</sup> In addition, in one part of the study, patients with adenocarcinoma of the lung or colon were treated with the radiolabeled version of conjugate **6b**. This radiolabeled conjugate provided definitive evidence of tumor localization in patients. Nevertheless, therapeutic activity was not noted with either of these conjugates. Also, a majority of patients in these trials developed an immune response both to the murine antibody and the Vinca component.

Unlike the conjugates described above, which were discontinued after Phase I evaluation, the antibody–doxorubicin conjugate BR96-Dox (**6d**), in which doxorubicin is linked to the chimeric BR96 antibody through an acid-labile hydrazone bond, was advanced to a Phase II human clinical trial in metastatic breast cancer.<sup>[38]</sup> In this randomized trial, patients were treated either with conjugate **6d** or with free doxorubicin. The toxicity profile of the conjugate was markedly different from that of the unconjugated doxorubicin, suggesting that antibody-mediated delivery can indeed

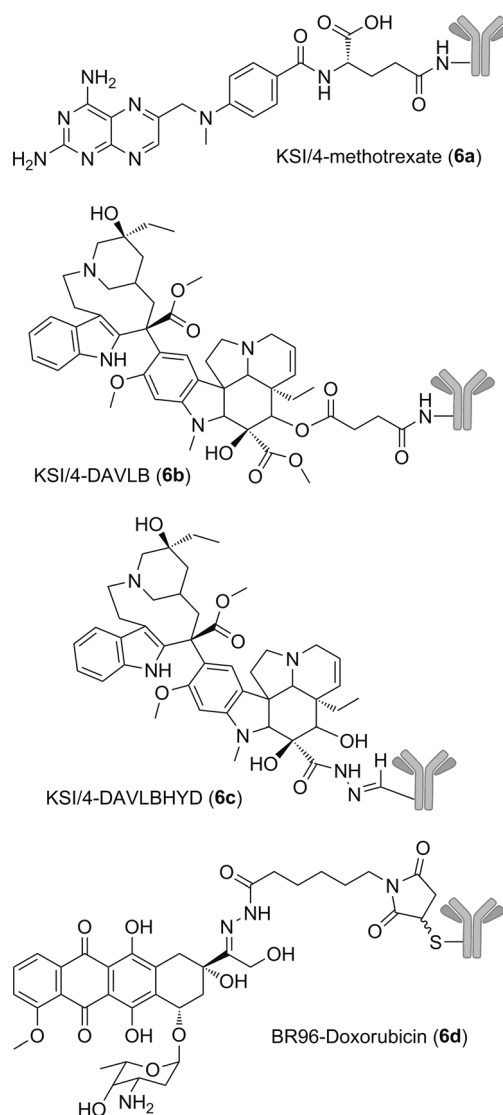


Figure 5. Structures of the first-generation antibody–drug conjugates.

alter the biodistribution of the drug. However, despite the strong preclinical data, wherein the conjugated doxorubicin was shown to be superior to free doxorubicin, the conjugate failed to demonstrate clinically meaningful therapeutic activity. Although BR96 was a chimeric antibody, the conjugate elicited an immune response in about 50% of the evaluable patients

#### 4. Improved Antibody–Drug Conjugates: Key Requirements

The lack of clinical success with early ADCs, all of which used existing anticancer drugs as the “payload”, initially dampened enthusiasm in this area of research. However, a careful analysis of each component of these early ADCs led to the identification of several factors that may have led to their failure.

#### 4.1. The Cytotoxic Molecule

A key feature of the early ADCs was their lack of sufficient *in vitro* potency, and the finding that conjugation often led to decreased potency compared to the parent free drug. For example the conjugate **6c** was reported to be eight times less potent than the unconjugated desacetylvinblastine drug.<sup>[33]</sup> Similarly, conjugate **6d** was about eight times less potent than doxorubicin.<sup>[34]</sup> The diminished potency upon conjugation can be attributed to the different modes of cellular uptake of the unconjugated and conjugated drug. A hydrophobic drug, such as vinblastine, can freely diffuse into the cell and get concentrated at its intracellular target (tubulin), resulting in cell death. The number of molecules of a moderately potent cytotoxic drug required to effect cell kill could be very high ( $> 10^6$  molecules/cell). Delivery of the cytotoxic molecule by an antibody is limited by two factors: a) moderate number of antigen molecules on the cell surface to which the antibody can bind (typically  $\approx 10^5$  receptors/cell), and b) internalization of cell-surface bound antigen–antibody complex, or intracellular processing to release the active drug moiety, may not be efficient. Thus, for an ADC to be therapeutically active, the number of molecules of the cytotoxic agent required to kill a cell has to be below, preferably well below, the number that is deliverable intracellularly by the antibody. Based on these calculations, cytotoxic molecules with potency in the picomolar range are required. Also, dosimetry studies with radiolabeled antibodies in cancer patients have revealed that uptake by the tumor was quite low (ranging from 0.003 to 0.01 % injected dose/gram of tumor).<sup>[39]</sup> In addition to high potency, an important requirement that is often overlooked is that cytotoxic molecules for use in ADCs have to be stable and adequately soluble in the aqueous milieu of the antibody. Another challenge is to be able to chemically modify the drug to introduce functional groups that are amenable to conjugation reactions with antibodies. The site and nature of the modification has to be carefully selected so as to preserve the potency of the parent drug.

#### 4.2. The Linker

In the first ADCs that entered clinical evaluation, the drug (methotrexate or desacetylvinblastine) bearing a carboxy group was merely mixed with the antibody in aqueous solution in the presence of the coupling agent EDC (*N*-ethyl-*N'*-(3-dimethylaminopropyl)carbodiimide hydrochloride) to enable amide bond formation with amino groups of the antibody. As antibodies possess amino acid residues with free carboxy groups (aspartate, glutamate) and free amino groups (lysine), EDC-mediated coupling can result in both intra- and intermolecular amide bond formation between amino acid residues of the antibody. Analytical tools were not available at that time to evaluate the biochemical characteristics of these conjugates prior to clinical evaluation. The first improvement in linker design came from the recognition that the linker should be cleaved upon internalization of the ADC into the targeted cell to release the active drug. In two of the

ADCs that entered the clinic, the drug (des-acetylvinblastine hydrazide and doxorubicin) was linked to the antibody through acid-labile hydrazone bonds to take advantage of the acidic pH value ( $\approx 5$ ) of the endosomes and lysosomes. Upon incubation of the ADC in acidic buffer, efficient release of the drug was demonstrated. However, incubation of the ADC under physiological conditions (pH 7.4, 37°C) resulted in a time-dependent slow release of drug.<sup>[33]</sup> Premature release of drug in circulation could lead to systemic toxicity and a lower therapeutic index. Thus, it was reasoned that an effective linker design has to balance the need of good stability during several days in circulation and efficient cleavage upon delivery into the target cell.

#### 4.3. The Antibody

The key function of the antibody is to preferentially bind to antigens on the target cell and thus concentrate the linked cytotoxic agent at the tumor site. Ideally, the antibody should be selected to cell-surface targets wherein the antigen is expressed in high copy numbers ( $> 10^5$ /cell). In addition, it is desirable for the antigen to be expressed homogeneously on all cells of the tumor, as determined by IHC staining of tumor tissue biopsies. The desired binding affinity of the antibody to its antigen is an issue of some debate. A high binding affinity ( $K_D < 1$  nM) may ensure good tumor localization, but some *in vivo* studies have suggested that antibodies with lower binding affinity may be able to penetrate solid tumors to a greater extent.<sup>[40]</sup> The relevance of these studies performed in mice bearing subcutaneous tumor xenografts to human cancers is not known. In addition to binding to the surface of tumor cells, the ability of the antibody–antigen complex to internalize into the cell to enable intracellular delivery of the linked payload is an important factor. This internalization process, called receptor-mediated endocytosis, is dependent on the nature of the antigen, with some growth factor receptors such as the epidermal growth factor receptor (EGFR) known to be well-internalized.<sup>[41]</sup> Thus, the efficiency of internalization is an important factor to consider in the selection of an antigen target for ADCs. While the ADC approach does not require that the antibody itself possesses functional activity, this feature of the antibody may confer additional therapeutic benefit. The problem of immunogenicity noted with early ADCs that used murine antibodies can be solved with the use of “humanized” or fully human antibodies that are now readily available.

### 5. Antimitotic Agents as ADC Payloads

Microtubule-acting compounds are antimitotic agents that interfere with the ability of mitotic spindles to segregate chromosomes and also alter the cytoskeletal architecture of cells, causing cell death.<sup>[42]</sup> The Vinca alkaloids (e.g. vincristine and vinblastine) are examples of tubulin-binding agents, which act by disrupting normal microtubule formation and dynamics, whereas the taxoids (e.g. paclitaxel and docetaxel) stabilize altered microtubule structures, thus interfering with



their normal degradation during cell division.<sup>[43]</sup> Because of their effect on mitosis, antimitotic agents are especially cytotoxic to cancer cells, which typically divide faster than most noncancerous cells. However, rapidly dividing noncancerous cells, such as the cells lining the intestines, cells in hair follicles, and myeloid cells, can also be killed, resulting in nausea, hair loss, and myelosuppression, respectively, as common side effects. Antimitotic agents that interfere with microtubule dynamics have also been found to impair the function of peripheral neurons, resulting in neuropathy.<sup>[44,45]</sup>

Most monoclonal antibodies and ADCs utilized for anticancer therapy target antigens that are over-expressed on the surface of cancer cells. However, the target antigens are also often expressed, to a lesser extent, on the surface of noncancerous cells. In addition, several types of noncancerous cells may also take up antibody or ADC by nonspecific pinocytosis or through cell surface Fc receptors.<sup>[46]</sup> It is therefore desirable to select a cytotoxic payload that shows some inherent selectivity toward killing cancerous cells versus noncancerous cells. Use of antimitotic agents as ADC payloads may partially achieve this goal by being less toxic toward slowly dividing or nondividing noncancerous cells that may be exposed to the conjugate.

The maytansinoid and auristatin microtubule binding agents possess the desired high potency for use in ADCs. Compounds from both classes have been successfully used as payloads for clinically approved ADCs, and are being tested in many ADCs in clinical trials.

### 5.1. Maytansinoids as ADC Payloads

Maytansine (**1**) is a benzoansamacrolide that was first isolated from the bark of the Ethiopian shrub *Maytenus ovatus* by Kupchan et al. in 1972.<sup>[4]</sup> Maytansine, and maytansinoids in general, bind to tubulin near the Vinca alkaloid binding site, and are thought to have a high affinity for tubulin located at the ends of microtubules, but lower affinity to sites distributed throughout the microtubules.<sup>[47]</sup> This binding results in the suppression of microtubule dynamics, causing cells to arrest in the G2/M phase of the cell cycle, resulting ultimately in cell death by apoptosis.

Maytansine was extensively evaluated in human clinical trials, but failed to demonstrate a therapeutic benefit at tolerable doses.<sup>[48]</sup> However, the unusually high cytotoxic activity of the maytansinoids makes them attractive candidates for antibody-targeted delivery. In addition, maytansine met other key criteria, such as good aqueous stability and reasonable aqueous solubility, for use as a payload for ADCs. Maytansine, however, does not possess an obvious functional group that can be used to link it to an antibody.

#### 5.1.2. Developing Linkable Maytansinoids

It was desired to link maytansinoids to antibodies in a manner that the resulting conjugate would be stable in circulation, yet cleavable in targeted cells. Disulfide linkages fit this criterion because they can be cleaved by thiols in the cytoplasm of the cell, which contains high levels of free thiol,

mainly in the form of glutathione (1–10 mM),<sup>[49]</sup> while blood contains much lower levels of free thiol ( $\approx 5 \mu\text{M}$ ).<sup>[50]</sup> Structure–activity relationship (SAR) studies on maytansinoids showed that several pharmacophores were required to maintain in vitro cytotoxicity.<sup>[51]</sup> The carbinolamide at C9 and the double bonds at C11 and C13 were required for activity. Also, loss of the epoxide moiety resulted in diminished activity. The ester side chain at C3 was required for biological activity, but the structure of this side chain could be varied without loss of potency. Since, the C3 position was amenable to modification, it was chosen for the incorporation of new ester side chains bearing a terminal thiol group to enable linkage to antibodies.<sup>[52]</sup>

Maytansinol (**7b**) is the hydrolysis product of **1** formed from cleavage of the ester group at C3. Maytansinol can be esterified with different side chains to produce maytansinoids of interest. Total syntheses of **7b** have been described that could potentially be adapted for the preparation of thiol-bearing maytansinoids.<sup>[53–55]</sup> However, this would be difficult, as the stereochemistry at several positions has to be maintained, and final yields from such multi-step syntheses are generally low. Thiol-bearing maytansinoids, such as DM1 (**7d**), are instead typically prepared through semisynthesis. The precursor, ansamitocin P-3 (**7a**), is obtained by fermentation of the microorganism *Actinosynnema pretiosum* (Figure 6).<sup>[52]</sup> Controlled reduction of **7a** with  $\text{LiAl}(\text{OMe})_3\text{H}$  gives maytansinol (**7b**). Esterification with a carboxylic acid that contains a disulfide, in the presence of a coupling agent (EDC) and a Lewis acid (zinc chloride) provides maytansi-

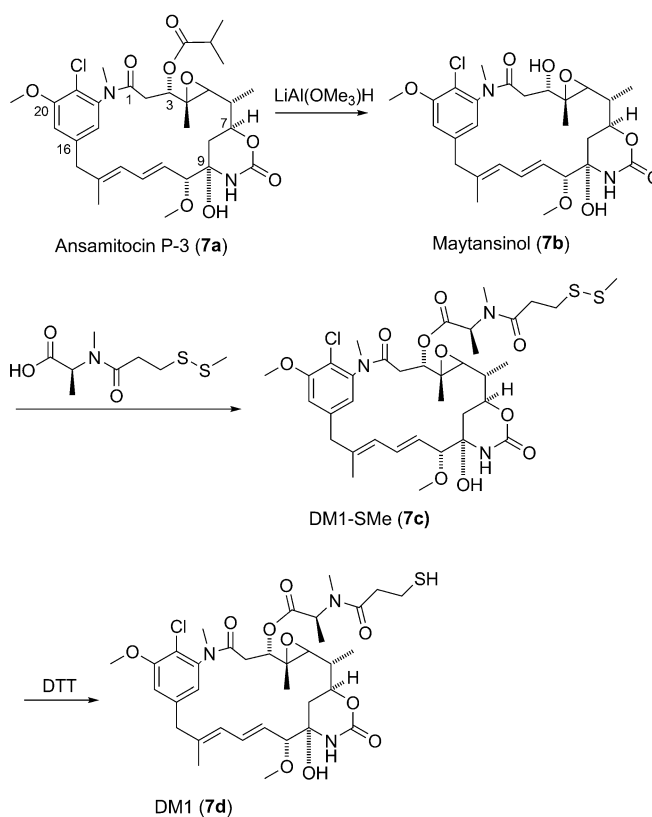
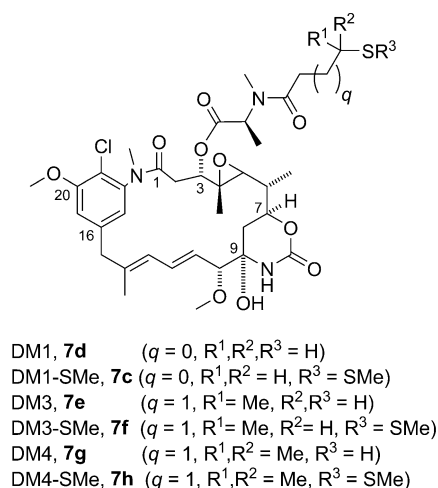


Figure 6. Semi-synthesis of DM1 from ansamitocin P-3.



**Figure 7.** Disulfide- and thiol-bearing maytansinoids.

noid disulfides (**7c**, **7f**, **7h**), which were reduced with dithiothreitol (DTT) to give the desired thiol-bearing maytansinoids (Figure 7, **7d**, **7e**, **7g**).

Typically, the *in vitro* cytotoxicity of maytansinoids is not determined on compounds that contain a thiol moiety, as these compounds can undergo thiol–disulfide exchange reactions with components of cell culture media, such as cystine. Instead, maytansinoid disulfide derivatives were used for cytotoxicity measurements. The maytansinoids DM1-SMe (**7c**), DM3-SMe (**7f**), and DM4-SMe (**7h**) had potencies ( $IC_{50}$  of 0.029 nM, 0.011 nM, and 0.0011 nM, respectively) that were comparable to, or higher than, that of maytansine ( $IC_{50} = 0.024$  nM) against KB cells. Similar results were also reported for the SK-Br-3 cell line.

### 5.1.3. Preparation of ADCs with Maytansinoids

Maytansinoid ADCs or antibody–maytansinoid conjugates (AMCs), wherein the maytansinoids are linked to antibodies through disulfide bonds, are generally prepared from a monoclonal antibody, a heterobifunctional linker, and a thiol-bearing maytansinoid, as shown in Figure 8.<sup>[52]</sup> Lysine residues of the antibody are reacted with the activated ester of a heterobifunctional linker to give a modified antibody that contains a reactive disulfide. The extent of modification can be varied by adjusting the molar equivalents of added linker. Typically, on average, three to four lysine residues on the antibody are modified. A thiol-bearing maytansinoid is then added to displace 2-thiopyridine to give the conjugate. The bond strength of the disulfide linkage can be varied by using maytansinoids or linkers that bear unhindered or sterically hindered thiols. AMCs can also be prepared by first reacting the thiol-bearing maytansinoid with the linker under highly concentrated conditions, and then reacting the resulting product with an antibody in aqueous solution. This second method is especially advantageous for forming AMCs bearing highly hindered disulfide bonds. AMCs with thioether linkages are prepared by reacting the antibody with a bifunctional linker composed of an activated ester and a maleimido group,

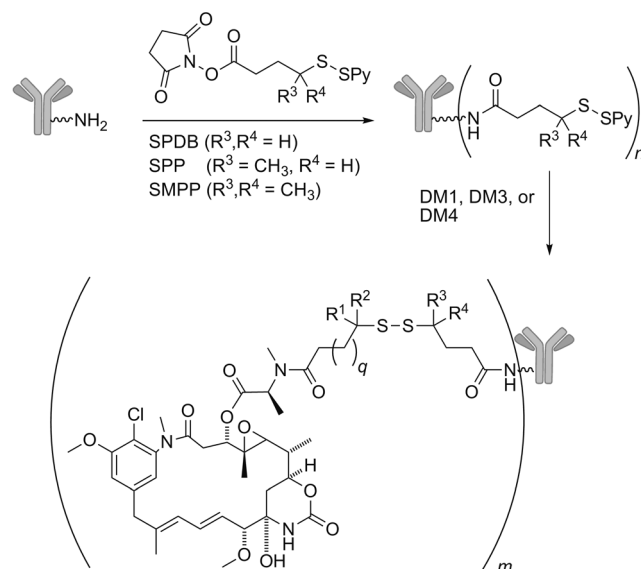


**Figure 8.** Conjugation of maytansinoids to antibodies by disulfide linkers.

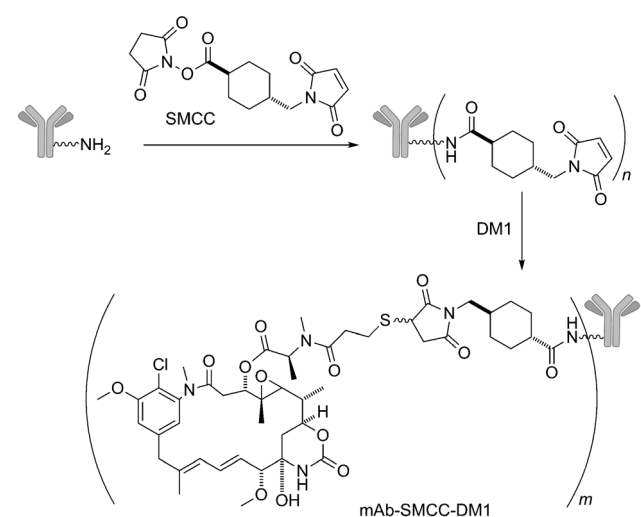


**Figure 9.** Conjugation of maytansinoids to antibodies by maleimide linkers.

such as SMCC, followed by reaction of the modified antibody with the thiol-containing maytansinoid (Figure 9).

In order to determine how the degree of steric hindrance of the disulfide bond would affect pharmacokinetics, several conjugates of the humanized C242 antibody were prepared.<sup>[56]</sup> Each conjugate was incubated with DTT at pH 6.5, 37°C to determine the relative rates of thiol-induced maytansinoid release *in vitro*. As expected, the more-hindered disulfide conjugates released maytansinoid at a slower rate than the less-hindered ones (Table 1). The most hindered AMC **8g** released maytansinoid over 22 000 times more slowly than **8a**, the least-hindered conjugate.

**Table 1:** Effect of hindrance on huC242 AMCs linker stability.<sup>[a]</sup>

Substituents						Disulfide hindrance	Disulfide reduction rate <sup>[b]</sup> ( <i>k</i> [M <sup>−1</sup> min <sup>−1</sup> ])	Relative stability	In vivo PK <i>t</i> <sub>1/2</sub> [h]
mAb side		DM side		<i>q</i>	ADC				
R1	R2	R3	R4						
H	H	H	H	0	<b>8 a</b>	0:0	14	1	15
Me	H	H	H	0	<b>8 b</b>	1:0	2	7	47
Me	Me	H	H	0	<b>8 c</b>	2:0	0.8	16	n.d.
H	H	Me	Me	1	<b>8 d</b>	0:2	1.0	14	87
Me	H	Me	H	1	<b>8 e</b>	1:1	0.8	170	n.d.
Me	H	Me	Me	1	<b>8 f</b>	1:2	0.014	980	218
Me	Me	Me	Me	1	<b>8 g</b>	2:2	< 0.00064	> 22 000	n.d.
H	H	Me	H	1	<b>8 h</b>	0:1	n.d.	n.d.	n.d.
–	–	–	–	–	<b>8 i</b>	thioether	n.d.	n.d.	n.d.

[a] n.d. = not determined; –: no disulfide present. [b] Conjugate disulfide reduction by DTT at pH 6.5, 37°C. Structures of disulfide AMCs are shown in Figure 8.

#### 5.1.4. In Vitro Cytotoxicity of AMCs

The in vitro cytotoxicity of a panel of conjugates of the huC242 antibody targeting the CanAg antigen, linked to maytansinoids using different disulfide linkers or a noncleavable thioether linker (Table 1), were tested against antigen-positive COLO 205 cells.<sup>[56]</sup> All of these conjugates were highly potent, regardless of linker structure, with  $\text{IC}_{50}$  values between 3.5–15 pM, thus disulfide cleavage was not required to kill these cells in vitro. The AMCs displayed poor potency toward antigen-negative cells, demonstrating the antigen specificity of the cytotoxic effect. A bystander killing assay was then performed, wherein a representative set of huC242 conjugates prepared with different linkers were incubated with antigen-negative (Namalwa) cells in the presence of different numbers of antigen-positive (COLO 205) cells. The AMCs with the disulfide linkers were able to kill the antigen-negative cells (also known as bystander cells) as long as enough antigen-positive cells were present (Figure 10). AMCs with steric hindrance on the maytansinoid side of the disulfide bond gave a higher degree of bystander killing. The AMCs **8h** and **8d** with hindrance on the maytansinoid side of the disulfide bond were found to have similar degrees of bystander killing. The AMC **8i** with the noncleavable thioether linker, however, had no bystander killing, as it could not kill antigen-negative cells, even when large amounts of antigen-positive cells were added.<sup>[57]</sup>

Although for huC242-AMCs, the nature of the linker did not affect in vitro potency against antigen-positive cells, this was often not the case for AMCs targeting other antigens. The in vitro potencies of AMCs prepared from an antibody against the folate receptor alpha (anti-FOLR1), illustrate this point (Figure 11).<sup>[58]</sup> The anti-FOLR1 conjugates with the thioether linker or disulfide linkers had similar in vitro potencies on antigen-positive KB cells, which express at least  $2 \times 10^6$  receptors per cell. Conjugates with disulfide linkers however were more potent than the AMC with the thioether linker against JEG-3 cells, which have lower levels of target antigen expression (about  $4 \times 10^4$  per cell).<sup>[58]</sup> Potency differences of disulfide-linked versus thioether-linked anti-FOLR1 AMCs therefore appear to be dependent on cell line and antigen expression levels. EGFR AMCs with a disulfide and thioether linker displayed similar potency

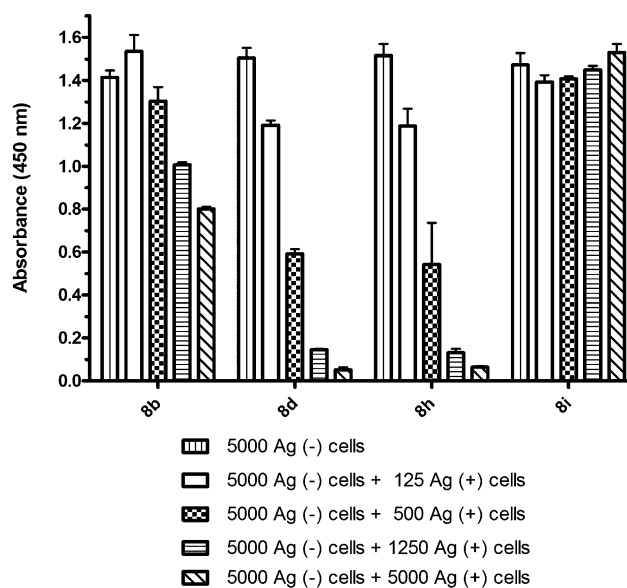


**Figure 10.** The effect of an AMC linkage on the killing bystander cells. Absorbance at 450 nm is a measure of cell viability. Cells were exposed to 1 nM conjugate for 5 days. Ag (–) = antigen-negative, Ag (+) = antigen-positive.

toward MDA-MB-468 cells, while the former was more than 20 times more potent toward A-431 cells, despite similar levels of antigen expression in this case.<sup>[59]</sup>

#### 5.1.5. Cellular Catabolism of AMCs

In order to understand the cytotoxicity and bystander killing data and to improve the design of AMC linkage systems, studies were conducted to elucidate the mechanism(s) of how AMCs are processed by antigen-positive cells.<sup>[60]</sup> Antigen-positive COLO 205 cells were treated in vitro with huC242- $^3\text{H}$ -maytansinoid conjugates prepared using different linkers (disulfide linkers: SPP, SPDB; thioether linker: SMCC; Figure 12). All conjugates gave lysine-bearing catabolites that had an intact linkage with the unaltered maytansinoids. The lysine-bearing catabolites were detected predominantly in the cell lysates and in smaller levels in the supernatants ( $\approx 10\%$  or less of the lysate level),

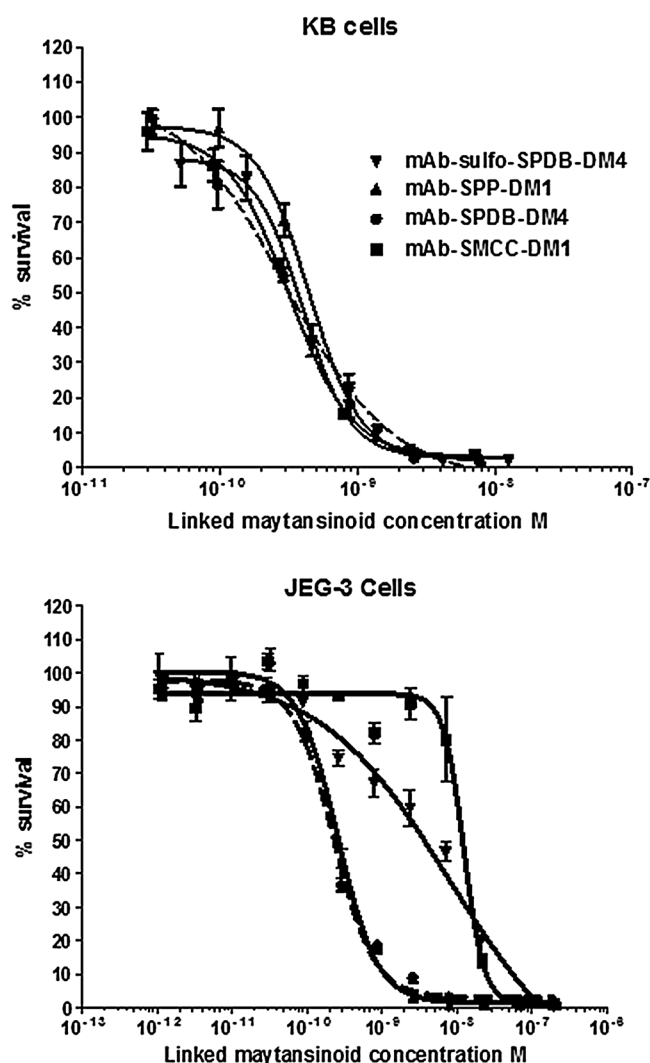


**Figure 11.** Cell-line dependency of the relative potency of Anti-FOLR1 AMCs in vitro.

suggesting that the antibody portion of the AMCs was fully degraded until only the lysine residue remained, and that these catabolites had some propensity to pass through cell membranes by either active or passive transport. The conjugate with a noncleavable thioether linker gave lysine-linker-maytansinoid as the sole catabolite, while the conjugates with disulfide linkers produced additional catabolites. The disulfide-linked DM1 conjugates generated DM1 and small amounts of *S*-methyl-DM1, which was presumably formed from DM1. Both DM1 and *S*-methyl-DM1 were detected in the cell culture medium as well as in the cell lysate. Likewise, the disulfide-linked DM4 conjugates generated DM4 and *S*-methyl-DM4 (the latter being the major species), which were also detected in both the culture medium and the cell lysate. No alteration of the macrocycle was detected in any of the catabolites, indicating that maytansinoids, even with their epoxide, ester, and cyclic carbamate moieties, are stable in lysosomes.

The proposed mechanism for the metabolism of each conjugate is shown Figure 13. After binding to the surface of

tumor cells and internalization, the antibody portion of the AMC is proteolytically degraded in the lysosome until only a residual lysine amino acid remains. The catabolite would then be passively or actively transported from the lysosome to the cytoplasm. In the case of AMCs with the noncleavable linker, the sole lysine-linker-maytansinoid catabolite produced can bind to tubulin in the cytoplasm to disrupt microtubule dynamics and induce cell killing, or it can be effluxed from the cell. Because lysine-bearing catabolites are charged, they would not be expected to diffuse into neighboring bystander cells to induce G2/M arrest and cell death. For AMCs with disulfide linkers, some of the initially generated lysine-bearing catabolite is cleaved by reduction in the cytoplasm to release the thiol-containing maytansinoids DM1 or DM4, which can be further *S*-methylated by an endogenous *S*-methyl transferase enzyme. Since these metabolites are uncharged, they are able to efflux out of the cell and diffuse into bystander cells to kill them. Bystander killing may be advantageous in several situations. It is suggested that ADCs may have poor penetration into tumors so that cancer cells that are progressively further away from a blood vessel may take up less conjugate.<sup>[61]</sup> However, noncharged low molecular weight metabolites may be able to penetrate deeper into tumors, thus killing tumor cells that are less accessible to the conjugate. Bystander killing may also be essential for killing heterogeneous tumors, which express high levels of target antigen on only a portion of the cells.

#### 5.1.6. Cytotoxicity of AMCs against MDR-1<sup>+</sup> Cells

There are several mechanisms by which tumor cells can become resistant to anticancer treatments. For example, multidrug-resistant (MDR) proteins can transport the chemotherapeutic agent out of the cells. One of the more prevalent MDR pumps is MDR-1. AMCs have been tested against cells that express the MDR-1 protein (also known as P-glycoprotein, or Pgp).<sup>[62]</sup> AMCs utilizing non-charged or non-polar linkers had lower in vitro potency against MDR-1<sup>+</sup> cells than against MDR-1<sup>-</sup> cells. MDR-1 is known in general to preferentially transport hydrophobic compounds more efficiently than hydrophilic compounds. Consequently, charged or hydrophilic linkers were developed and the AMCs prepared from them were shown to produce highly charged or polar metabolites, resulting in improved potency against MDR-1<sup>+</sup> cells. Sulfo-SPDB and Mal-PEG4-NHS are examples of polar linkers (Figure 14).<sup>[62,63]</sup>

#### 5.1.7. Preclinical Pharmacokinetics, Tolerability, and Efficacy of AMCs

The AMCs prepared with cleavable disulfide linkers and noncleavable thioether linker were evaluated in vivo to determine their pharmacokinetic (PK) parameters.<sup>[56]</sup> The circulation half-life of AMCs with disulfide linkers was dependent on the degree of steric hindrance of the disulfide linkage; as hindrance was increased, the clearance rate was progressively decreased (Table 1). For example, the highly hindered AMC **8f** had a half-life of about 218 hours, which was comparable to that of the noncleavable AMC **8i** and that



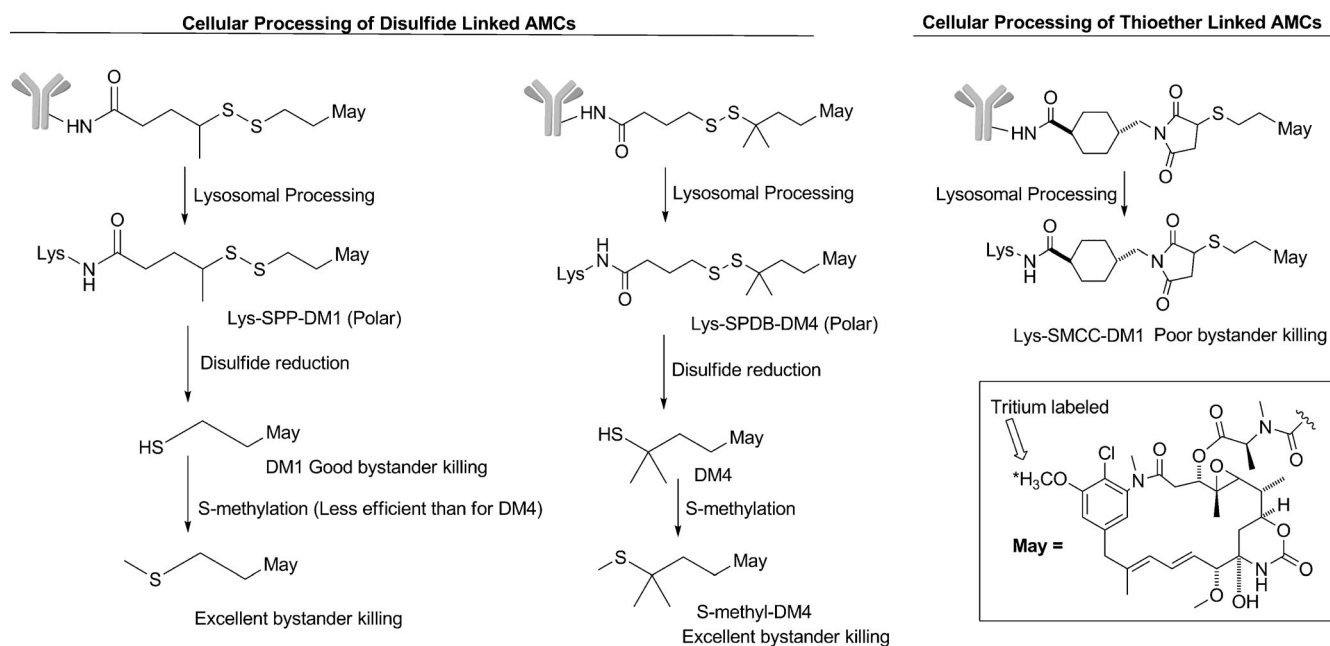


Figure 12. Cellular processing of AMCs.

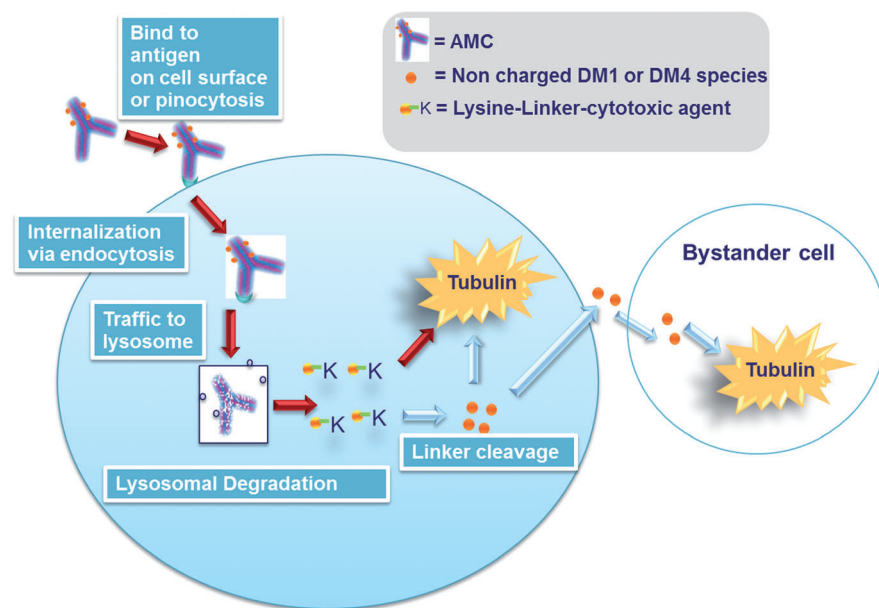


Figure 13. Proposed mechanism for AMC catabolism and potential bystander cell killing.

of unmodified human IgG<sub>1</sub> in mice. The half-life of **8f** was 14.5 times longer than that of the unhindered AMC **8a** in vivo. Tolerability of AMCs with disulfide linkers in mice, however, was not greatly affected by hindrance of the disulfide linker, because the different disulfide-linked AMCs had similar MTDs of about 50 mg kg<sup>-1</sup> (antibody dose at a typical maytansinoid loading of 3.5 to 4 per antibody).<sup>[56]</sup> AMCs made with noncleavable linkers were better tolerated in mice, with MTDs that were 2 to 3 times higher than those of AMCs with disulfide linkers.<sup>[62]</sup>

efficacy, and that the location of the hindrance also affected efficacy. In particular, hindrance on the maytansinoid side of the disulfide bond gave improved efficacy as compared to hindrance on the antibody side. This improved activity can be attributed to the generation of a more potent maytansinoid metabolite, although some differences in AMC processing and pharmacokinetics may also play a role.

Although in a majority of cases an AMC with the optimal disulfide linker is more active in vivo than the corresponding conjugate with a noncleavable linker,<sup>[56, 64]</sup> there may be some

In vivo experiments with AMCs linked through thioether or disulfide bonds showed that efficacy often does not correlate with in vivo stability. The antitumor activity of huC242–maytansinoid conjugates with varying steric hindrance in the disulfide link (**8b**, **8e**, **8f**) was compared in mice bearing COLO 205 xenografts (Figure 15). In this model, the AMC **8b** showed the best efficacy. At the tested dose, AMCs with less readily cleavable linkages had little or no efficacy advantage over mice dosed with a phosphate-buffered saline (PBS) control. In a second experiment, groups of mice bearing COLO 205 xenografts were treated with another set of AMCs (Figure 16). The AMC **8d** was the most efficacious, followed by **8h**, while **8b** and **8c** were the least efficacious. These two sets of experiments indicate that extensive disulfide hindrance could be detrimental to AMC

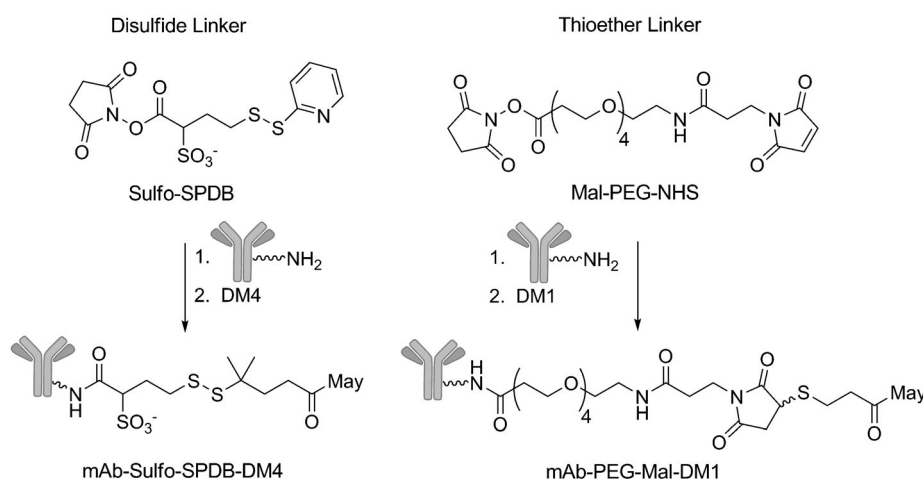


**Figure 14.** Polar sulfo-SPDB and mal-PEG4-OSu linkers, and the ADCs prepared from them.

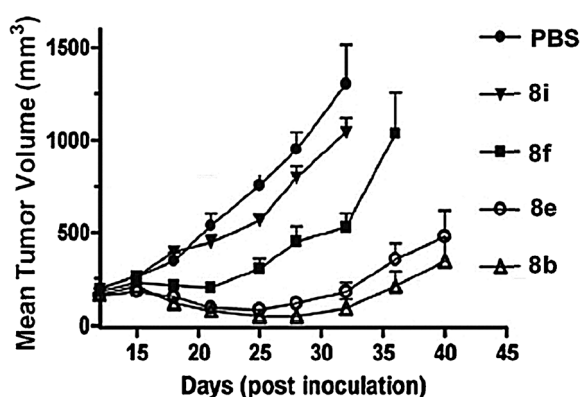


**Figure 15.** Effect of disulfide hindrance on the in vivo efficacy of huC242 conjugates on COLO 205 xenografts.

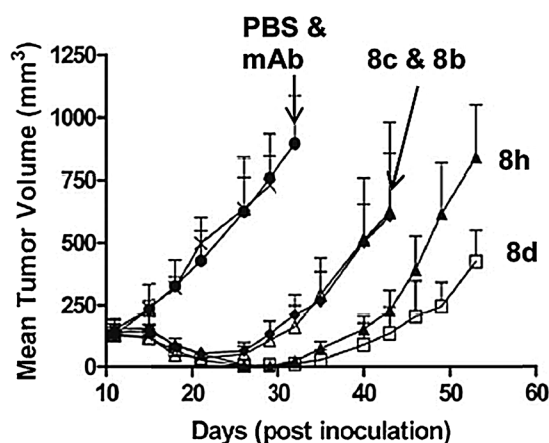


**Figure 16.** Effect of hindrance at different sides of the AMC disulfide linkage on in vivo efficacy.

target dependency. For example, conjugates of the anti-HER2 antibody trastuzumab linked to the maytansinoid DM1 through a disulfide linker or a thioether linker showed similar in vivo efficacy.<sup>[65]</sup>

### 5.1.8. Studies on the In Vivo Metabolism of ADCs and Cytotoxicity of Catabolites

For in vivo investigations, tumor-bearing mice were separately dosed with huC242-<sup>[3</sup>H]maytansinoid conjugates that were prepared using different linkers (disulfide linkers: SPP, SPDB; thioether linker: SMCC).<sup>[66]</sup> The mice were sacrificed after intervals of between 2 hours and 7 days post-dosing, then the tumors and livers were excised and homogenized, and the radiolabeled species were analyzed by HPLC. As noted with the in vitro metabolism experiments, lysine-linker-maytansinoid (Lys-SMCC-DM1) was the sole catabolite detected for the conjugate with the noncleavable linker (mAb-SMCC-DM1) at any time point. The lack of new catabolites in liver or bile indicated that no phase I or phase II liver metabolism occurred to any significant extent. In mice treated with conjugates that bear the disulfide linkers, the catabolite profile from the tumors matched that seen in the in vitro studies. In liver, additional catabolites that consist of the oxidation products *S*-methyl-DM1 sulfoxide and *S*-methyl-DM1 sulfone were formed from DM1 disulfide-linked ADCs, while *S*-methyl-DM4 sulfoxide and *S*-methyl-DM4 sulfone were formed from DM4 disulfide-linked ADCs (Figure 17).<sup>[66]</sup> Again, no phase II metabolites were detected in these liver homogenates.

The catabolites and the liver-oxidized metabolites, which are formed from ADCs in vivo, can potentially contribute to systemic toxicity. It is therefore desirable to know the cytotoxicity of each species and determine if liver metabolism effectively detoxifies catabolites. All of the lysine-bearing catabolites had relatively poor cytotoxic potency in vitro (Table 2). However, these catabolites appear to be highly potent if delivered into a cell by AMC processing. The noncharged catabolites DM1 (7d), *S*-methyl-DM1, DM4 (7g), and *S*-methyl-DM4 were highly cytotoxic compounds, while the sulfoxides and sulfones of *S*-methyl DM1 and *S*-methyl DM4 had relatively weak cytotoxicities, suggesting that mouse liver efficiently detoxifies these catabolites through oxidation. Also, the lysine-bearing catabolites generated from ADCs with noncleavable linkers are not altered in the liver, thus retaining their relatively poor cytotoxicity.

The catabolites and the liver-oxidized metabolites, which are formed from ADCs in vivo, can potentially contribute to systemic toxicity. It is therefore desirable to know the cytotoxicity of each species and determine if liver metabolism effectively detoxifies catabolites. All of the lysine-bearing catabolites had relatively poor cytotoxic potency in vitro (Table 2). However, these catabolites appear to be highly potent if delivered into a cell by AMC processing. The noncharged catabolites DM1 (7d), *S*-methyl-DM1, DM4 (7g), and *S*-methyl-DM4 were highly cytotoxic compounds, while the sulfoxides and sulfones of *S*-methyl DM1 and *S*-methyl DM4 had relatively weak cytotoxicities, suggesting that mouse liver efficiently detoxifies these catabolites through oxidation. Also, the lysine-bearing catabolites generated from ADCs with noncleavable linkers are not altered in the liver, thus retaining their relatively poor cytotoxicity.

### 5.2. Auristatin Analogues as ADC Payloads

The small linear peptide dolastatin 10 (2a) (Figure 2) is a highly potent antimitotic agent that was isolated from the marine shell-less mollusk *Dolabella auricularia* found in the Indian Ocean and the coastal waters of Japan.<sup>[67]</sup> Dolastatin 10 and its derivatives have been shown to inhibit tubulin-

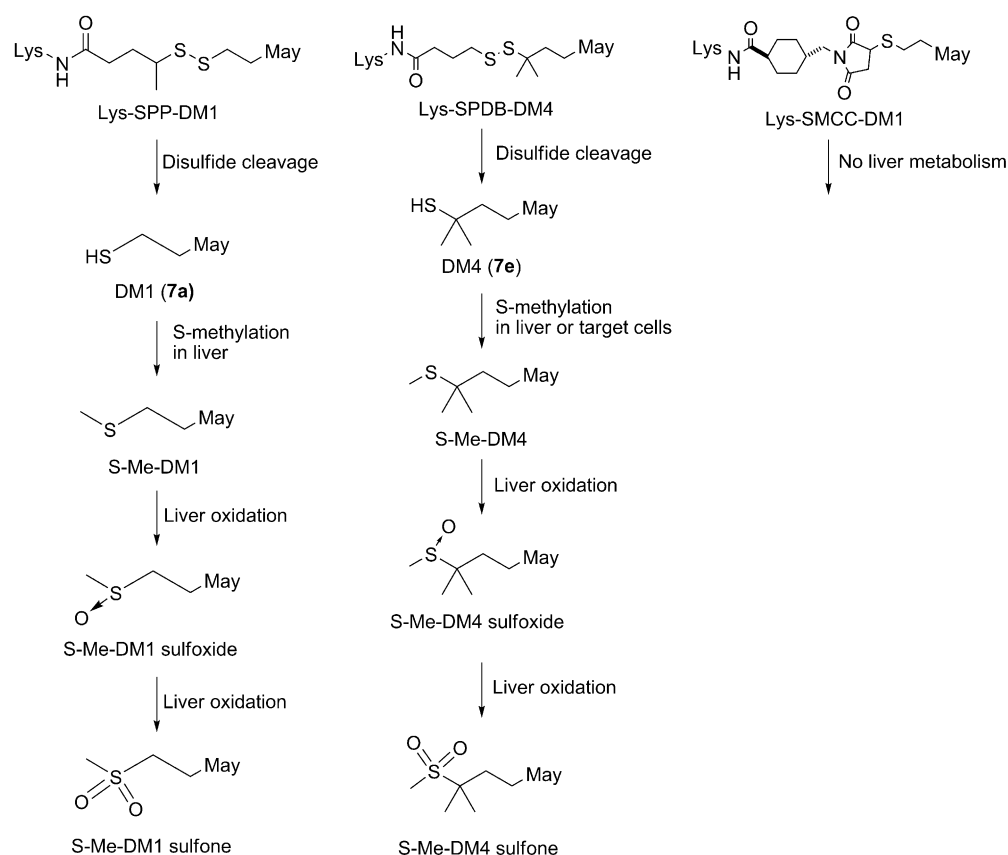


**Figure 17.** Liver metabolism of the lysosomal and S-methylated catabolites of AMCs.

dependent GTP binding, cause noncompetitive inhibition of vincristine binding to tubulin, and inhibit microtubule dynamics. Some dolastatins, such as dolastatin 15 (**2b**) and the synthetic analogue Cemadotin (**2c**) are known to be labile to proteases and esterases, as shown in Figure 18. Such labile dolastatins may not be desirable for use as ADC payloads, as they could be fully or partially inactivated when processed in the lysosomes of targeted cells.

the methyl ester derivative of MMAF (MMAF-OMe) is one of the most cytotoxic auristatin compounds and is approximately 100 times more cytotoxic than MMAE on most of the tested cell lines. It is believed that MMAF-OMe can diffuse into cells where esterases in the cytoplasm convert it into MMAF. Thus it is suggested that MMAF has low cytotoxicity because its charged carboxy group hinders diffusion into cells,

### 5.2.1. Developing Linkable Auristatins

The auristatin series of antimetabolic agents are fully synthetic compounds that were identified by SAR studies based on dolastatin 10.<sup>[68]</sup> The dolaphenine residue of **2a** could be replaced with phenethyl amine or substituted phenethyl amine moieties without loss of potency. It was also found that potency was retained when the terminal tertiary amine moiety of dolastatin was replaced with a primary or secondary amine. Monomethyl auristatin E (MMAE, **9a**) and monomethyl auristatin F (MMAF, **9b**) were prepared from such SAR studies and then derivatized for use as payloads for ADC (Figure 19).

MMAF is approximately 100 times less cytotoxic in vitro than MMAE.<sup>[69]</sup> Nevertheless,

**Table 2:** In vitro cytotoxicity of AMC catabolites and liver oxidation products.

ADC catabolite	IC <sub>50</sub> [M] (KB)	liver metabolite(s) formed from AMC catabolites	IC <sub>50</sub> [M] (KB)	Decrease in potency <sup>[c]</sup>
S-Me-DM1	6.6 × 10 <sup>-11</sup>	S-Me-DM1 sulfoxide	1.3 × 10 <sup>-8</sup>	196
		S-Me-DM1 sulfone	3.5 × 10 <sup>-9</sup>	53
S-Me-DM4	2.6 × 10 <sup>-11</sup>	S-Me-DM4 sulfoxide	1.9 × 10 <sup>-9</sup>	73
		S-Me-DM4 sulfone	8.0 × 10 <sup>-10</sup>	31
DM1	1.0 × 10 <sup>-9</sup> <sup>[b]</sup>	DM1 sulfinic acid	n.d.	n.d.
		DM1 sulfonic acid	4.0 × 10 <sup>-8</sup>	40
DM4	3.0 × 10 <sup>-10</sup> <sup>[b]</sup>	DM4 sulfinic acid	n.d.	n.d.
		DM4 sulfonic acid	2.7 × 10 <sup>-8</sup>	90
Lys-SPP-DM1	2.9 × 10 <sup>-8</sup>	–	–	–
Lys-SPDB-DM4	3.3 × 10 <sup>-8</sup>	–	–	–
Lys-SMCC-DM1	6.2 × 10 <sup>-8</sup>	–	–	–

[a] ND: Not determined; the compound has not been synthesized. – Indicates no value because parent compounds were not metabolized. (KB) indicates that the cytotoxicity of the various maytansinoids was determined on the KB cell line. [b] In vitro cytotoxicity varies due to thiol reactivity with cystine and other disulfide-containing components present in the cell media. [c] Fold decrease in potency = (IC<sub>50</sub> liver metabolite)/(IC<sub>50</sub> primary metabolite).

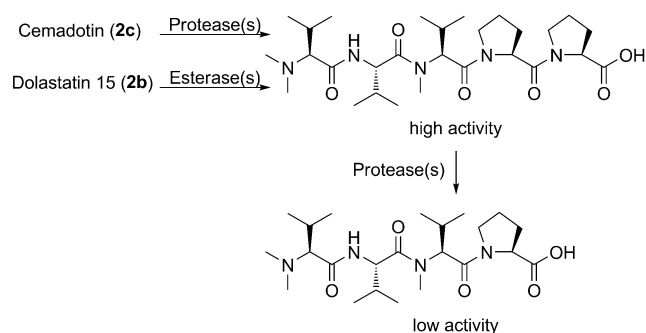


**Figure 18.** Proteolytic inactivation of the active moiety derived from cemadotin (**2c**) and dolastatin 15 (**2b**).

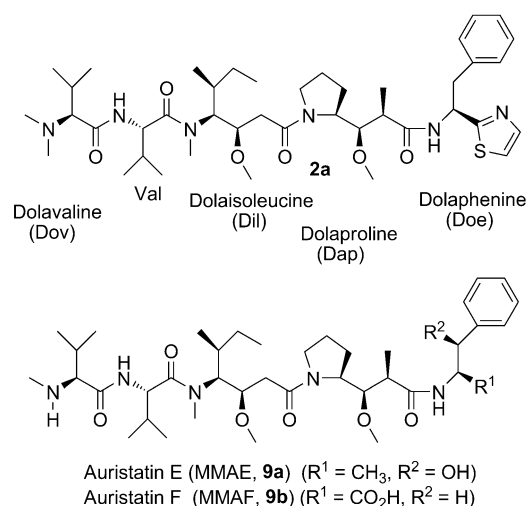


**Figure 19.** Named moieties for SAR studies on dolastatin 10 (**2a**) and structures of MMAE and MMAF.

but once inside a cell, it would be very potent. MMAE and MMAF were selected and modified for linkage to antibodies.

MMAE is typically modified at its terminal amine so that it can be linked to an antibody through a dipeptide attached to a *para*-aminobenzyl (PAB) moiety (Figure 20). The maleimide moiety of the derivative allows the compound to be linked to a thiol group on a targeting agent. Valine–citrulline–PAB constructs are known to be cleaved by cathepsin B, and all of the auristatin E ADCs presently in clinical trials utilize valine–citrulline (val-cit) as the dipeptide linker. Auristatin E analogues that do not contain a peptide linker have also been reported, but ADCs of these compounds have not yet advanced to the clinic. MMAF has been derivatized on the terminal secondary amine with the same mal-caproyl-val-cit linkage system and also with a noncleavable maleimide-caproyl linker. Auristatin F analogues that bear a terminal dimethyl amine substituent have also been modified at the carboxy terminus for linkage to antibodies, but these will not be discussed here.<sup>[70]</sup>

### 5.2.2. Preparation of Auristatin-ADCs

Free thiol moieties on the antibody are required to enable conjugation to maleimide-bearing auristatin derivatives. However, antibodies do not generally contain free thiols, but they do contain endogenous cysteine residues that exist as disulfide pairs with other cysteines to form 4 interchain and 12 intrachain

disulfide bonds (for a human IgG<sub>1</sub> antibody). The interchain disulfides can be reduced and maintained in a reduced state more easily than the intrachain disulfides.<sup>[71]</sup> The interchain disulfide bonds can be fully or partially reduced by a mild reducing agent such as DTT to give a distribution of antibody

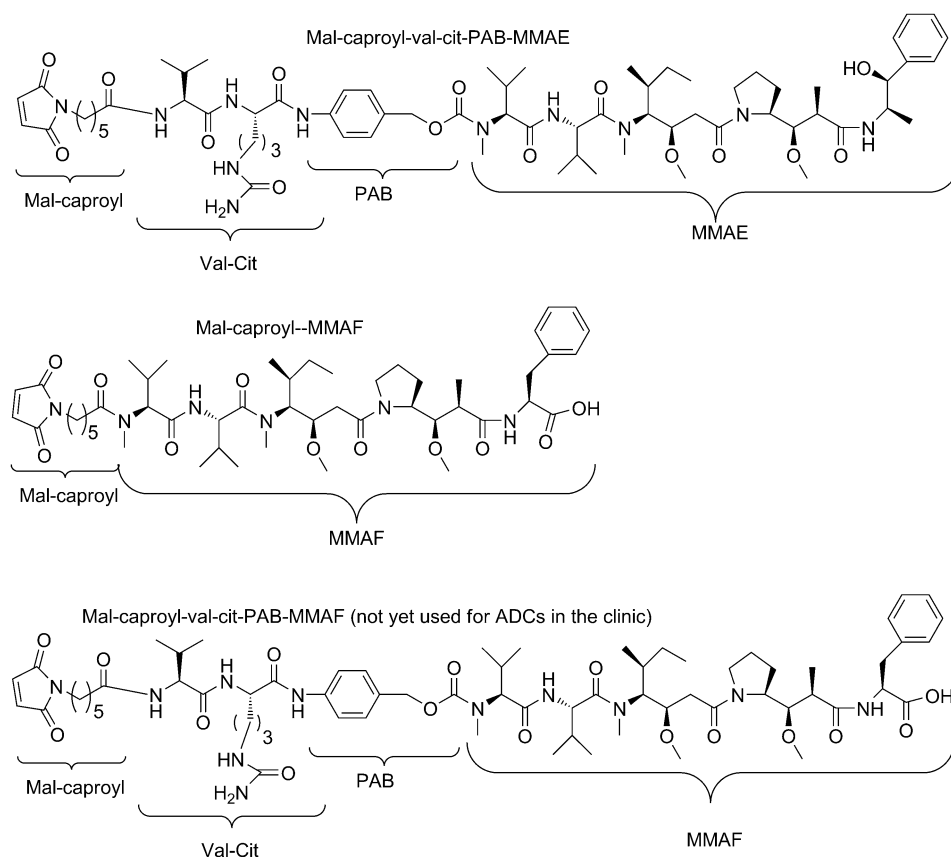


**Figure 20.** Selected linkable derivatives of MMAE and MMAF.



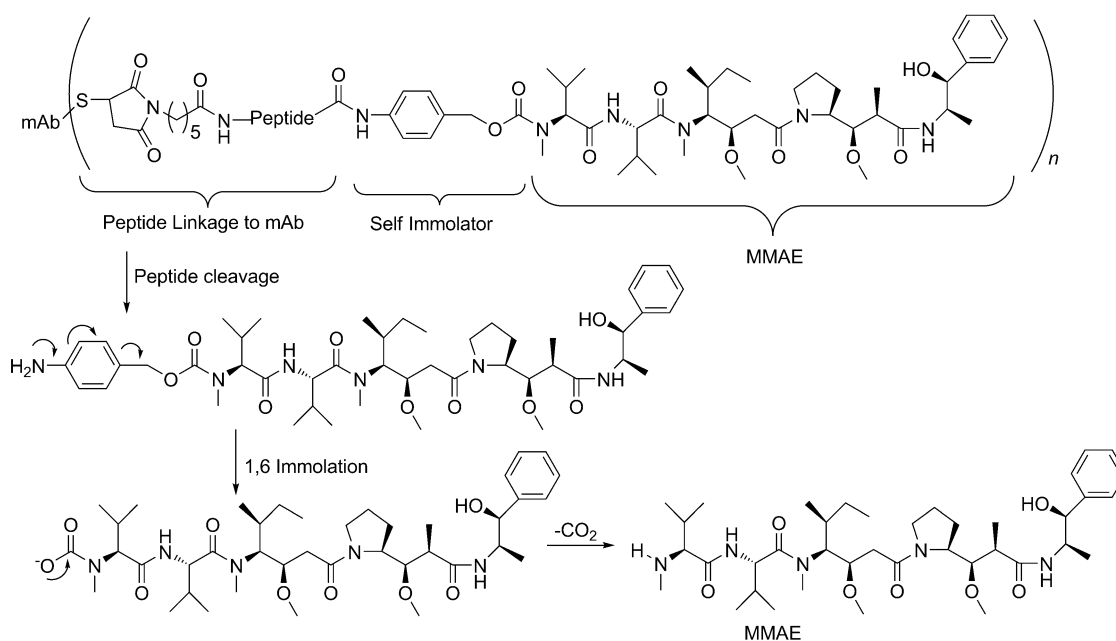


**Figure 21.** Cellular metabolism of self-immolative ADCs containing auristatin E.

species with two to eight free thiol groups. The reduced antibody with its newly freed thiol groups can then be purified to remove reducing agent and reacted with a maleimide-containing auristatin derivative. Conjugates with a varying distribution of auristatin molecules per antibody were obtained, with an average of four auristatins linked per antibody.<sup>[72]</sup> Conjugates of MMAE utilizing the val-cit linkage have also been purified by hydrophobic-interaction chromatography (HIC) to separate individual species with two, four, or eight MMAEs per antibody.<sup>[73]</sup> The separated species have been used for research, but have not yet been evaluated in the clinic.

### 5.2.3. Cytotoxicity of Auristatin-ADCs

Studies were conducted to determine how the load of MMAE on an antibody would affect the in vitro and in vivo potency of the resulting conjugate, as well as pharmacokinetic parameters.<sup>[73]</sup> Anti-CD30 antibody–MMAE conjugates that bear the separated species with two, four, or eight MMAE molecules per antibody retained full binding affinity to the antigen. Cytotoxicity assays indicated a small increase in the in vitro potency as the MMAE load increased.

ADCs of MMAF have also been reported to be highly cytotoxic to antigen-positive cells. The anti-CD30 antibody cAC10 was separately conjugated to mal-caproyl-vc-PAB-MMAF and mal-caproyl-MMAF to give an ADC with a protease cleavable linkage and an ADC with a noncleavable linkage, respectively. The two ADCs displayed a similar level of potency against a panel of CD30-positive cell lines. However, the val-cit-linked ADC was reported to be up to 10 times more potent on some cell types. It was proposed that MMAF ADCs utilizing val-cit linkages may, in some cases, release catabolite more efficiently than MMAF ADCs using the noncleavable linker.<sup>[69]</sup>

### 5.2.4. Cellular Catabolism of Auristatin ADCs

As is the case with AMCs, auristatin ADCs are also catabolized by target cells. The proposed mechanism for the catabolism of MMAE ADCs is shown in Figure 21. The antibody component of auristatin ADCs binds to a targeted antigen on the surface of cells, after which the conjugate is internalized and routed to a proteolytic compartment. Cleavage of the amide bond between the peptide and the aromatic amine followed by self-immolation of the *para*-aminobenzyl (PAB) moiety with loss of carbon dioxide gives MMAE. MMAF is most often conjugated to an antibody through a noncleavable linker, thus the linker moiety of these ADCs is not cleaved in catabolic vesicles of cells (Figure 22). Instead, the antibody portion of the resulting ADC is degraded to release a catabolite that contains MMAF linked to cysteine (cys-mal-caproyl-MMAF).

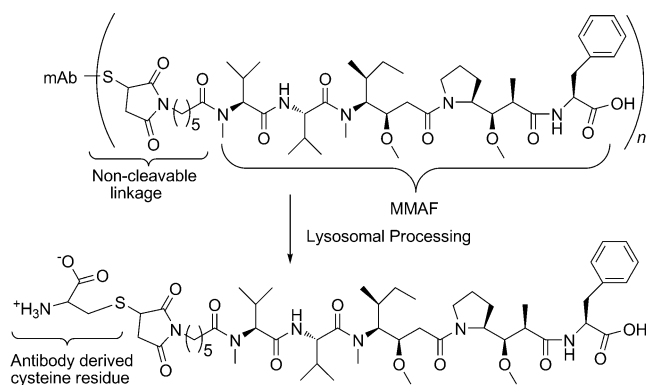


**Figure 22.** Cellular metabolism of ADCs containing noncleavably linked auristatin F.

Protease-labile self-immolative conjugates of MMAE ADCs can induce bystander killing presumably by releasing membrane permeable MMAE, which can diffuse into and kill proximal cells.<sup>[74]</sup> However, MMAF conjugates linked through a noncleavable linker do not induce bystander killing, presumably because they release the charged cyclopropyl-MMAF catabolite, which is poorly membrane permeable.

The efficiency of ADC internalization is expected to impact potency, but the route by which an ADC is internalized appears to also determine if potent catabolites are released. Smith et al. conducted a study with the ADC L49-MMAF, in which the antimelanotransferrin monoclonal antibody (L49) was linked to MMAF by a noncleavable linker.<sup>[75]</sup> The ADC was readily internalized by several antigen-positive cell lines, which had high target antigen expression. The cell lines were also sensitive to membrane-permeable auristatins, so it was expected that the L49 ADC would be highly cytotoxic to all of these targeted cells. Some cell lines, however, were resistant to the L49-MMAF. It was later determined that insensitive cells were internalizing L49 into vesicles known as caveolae, and the ADC apparently was never routed to catabolic vesicles. Without ADC degradation, cytotoxic catabolites could not be released to kill the cells.

### 5.2.5. Preclinical Pharmacokinetics, Tolerability, and Efficacy of Auristatin ADCs

Since, the cAC10 conjugate that bears eight MMAE was more potent in vitro than conjugates with a lower MMAE load, an in vivo evaluation was conducted. However, the ADC with eight MMAE per antibody was found to clear from circulation substantially faster than the conjugates containing four or fewer MMAE molecules per antibody.<sup>[73]</sup> This is often referenced as proof that ADCs with a high drug load will be cleared rapidly. However, interchain disulfide bonds covalently hold together the heavy and light chains of the antibody, thus contributing to antibody stability, so the cleavage of all these disulfide bonds to provide attachment sites for a higher load of MMAE has the potential to alter the stability of the conjugate and the in vivo clearance rate. More studies with different linkage systems or cytotoxic molecules may be required to determine if high-drug-load ADCs can be prepared without compromising in vivo clearance rates. The cAC10 ADCs that bear four MMAE molecules per antibody have an MTD of between 30–40 mg kg<sup>-1</sup> (antibody protein dose) in SCID mice.<sup>[71]</sup>

Conjugates of cAC10 with val-cit-linked MMAF or mal-caproyl-MMAF had similar in vivo efficacy against Karpas 299 xenografts in nude mice. However, the ADC with the noncleavable mal-caproyl linker had an MTD in mice of greater than 150 mg kg<sup>-1</sup>, while the ADC linked by the cleavable val-cit linker was three times more toxic, with an MTD of 50 mg kg<sup>-1</sup>, with an MMAF load of four per antibody. SGN-75 is an anti-CD70 antibody linked to MMAF by a noncleavable linker. For in vivo studies, a version of SGN-75 that was dual radiolabeled ([<sup>14</sup>C]-MMAF and [<sup>3</sup>H]-anti-CD70 antibody) was prepared.<sup>[76]</sup> Biodistribution studies in tumor-bearing mice were conducted with this conjugate and

accumulation of <sup>14</sup>C from MMAF or <sup>3</sup>H from antibody were determined for tumor and various normal tissues. Radioactivity derived from MMAF was found to preferentially accumulate in the tumor (82 % injected dose/g after 2 days). Also, similar to maytansinoid conjugates, the radiolabeled MMAF ADC was highly accumulated in tissues that catabolize antibodies.

## 6. DNA Agents as ADC Payloads

### 6.1. Calicheamicins

The calicheamicins are a class of enediyne-containing antitumor antibiotics that are recognized as being among the most potent antitumor agents ever discovered. They were first identified in 1986 as a fermentation product of the bacterium *Micromonospora echinospora* ssp. *calichensis* through a screening effort to discover new DNA-damaging agents.<sup>[77,78]</sup> Calicheamicin  $\beta_1^{\text{Br}}$  (**10a**) and  $\gamma_1^{\text{Br}}$  (**10b**) were the first members of this class to be isolated, followed by calicheamicin  $\gamma_1^{\text{I}}$  (**10c**; Figure 23) and other calicheamicins.<sup>[79]</sup>

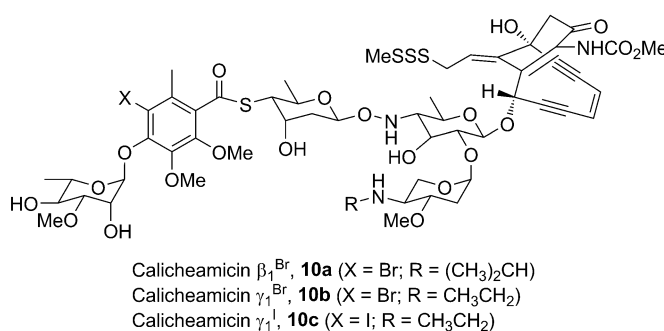
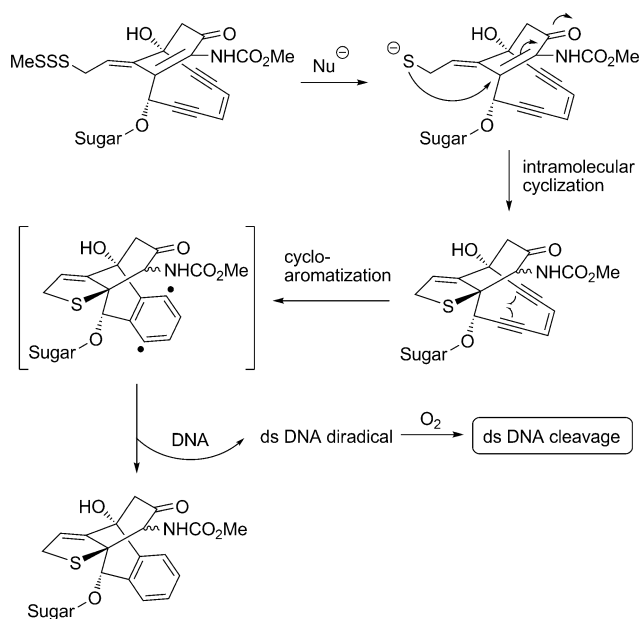


Figure 23. Structures of calicheamicins.

Calicheamicin  $\gamma_1^{\text{I}}$ , the most prominent member of this family, is structurally complex, possessing a highly functionalized bicyclic enediyne unit with a methyl trisulfide moiety bridged through a series of unusual linkages to an extended sugar residue, which possesses a fully substituted benzene ring. It was found to possess exquisite potency in vivo against a variety of tumor types at doses as low as 0.15  $\mu\text{g kg}^{-1}$ .<sup>[80]</sup> In spite of the molecular complexity, all of these elements work together to give the calicheamicins a fascinating mechanism of action (Figure 24).<sup>[81,82]</sup> The aryl tetrasaccharide of **10c** serves to direct the molecule by binding tightly within the minor groove of DNA in a relatively sequence-specific manner, thus positioning the enediyne warhead within the DNA double helix. In this position, the methyl trisulfide is available to undergo nucleophilic attack (e.g. glutathione) ultimately releasing a free thiol, which spontaneously cyclizes into the  $\alpha,\beta$ -unsaturated ketone bridgehead of the enediyne. The resulting angular strain imposed on the enediyne through this addition is relieved through a cycloaromatization (Bergman type)<sup>[83]</sup> reaction, which generates a 1,4-benzene dirad-



**Figure 24.** Mechanism of DNA cleavage by calicheamicin.

ical. The diradical thus formed abstracts hydrogen atoms from both strands of the duplex DNA, resulting in a double-stranded DNA diradical, which in the presence of oxygen leads to cleavage of DNA double strands and subsequent cell death.

As a result of this unique mechanism of action and high potency, multiple analogues of the calicheamicins have been explored as potential anticancer agents in preclinical models. However, because of the prevalence of associated toxicities upon treatment with these compounds, calicheamicin therapies as single agents have not been developed. In spite of this, their high potency makes them ideal candidates for ADCs, particularly where antigen expression is limited.

#### 6.1.1. Calicheamicins as ADC Payloads

Calicheamicin  $\gamma_1^1$  was considered too toxic for use in an antibody–drug conjugate because of its high potency and toxicity, which eventually led to the development of *N*-acetyl  $\gamma$  calicheamicin, a 20 times less potent analogue, as the choice for the calicheamicin core.<sup>[84]</sup> Additionally, the natural trisulfide found in the calicheamicin structure was converted to a disulfide, thus incorporating a functional group that allows conjugation to an antibody. Efforts to prepare calicheamicin–antibody conjugates primarily focused on using either a hydrazone or an amide linkage.<sup>[85]</sup>

Conjugates with linkable forms of calicheamicin (Figure 25) have been prepared with the anti-MUC1 and anti-CD33 antibodies with strikingly different outcomes.<sup>[85–88]</sup> In one method of conjugation, NAc- $\gamma$  calicheamicin-DMH (**10d**) was linked to the antibody through an acid-labile hydrazone bond. Formation of this bond was accomplished by oxidizing carbohydrate residues of the antibody with periodate to generate aldehyde groups, followed by reaction with **10d** to generate a “carbohydrate conjugate”. Alternatively, an

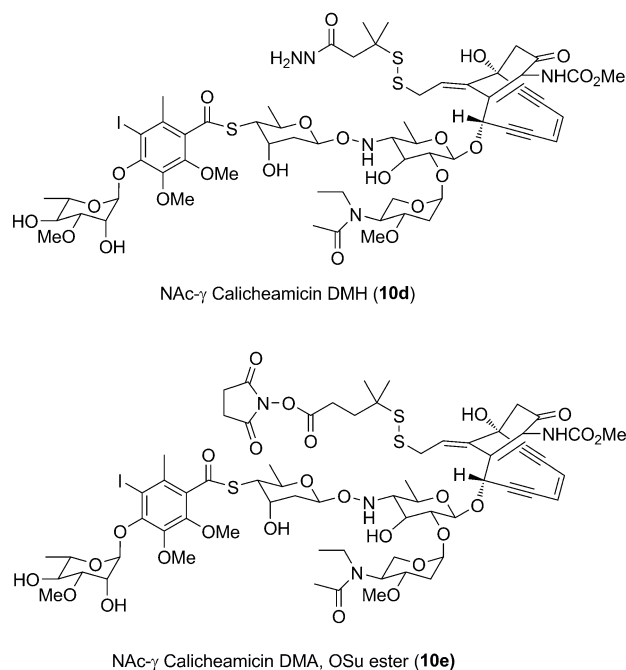


**Figure 25.** Structures of linkable NAc- $\gamma$  calicheamicin DMH (**10d**) and DMA, OSu ester (**10e**).

“amide conjugate” was prepared by linking NAc- $\gamma$  calicheamicin-DMA (**10e**) by a lysine group on the antibody, thus creating a more stable linkage. While each of these linkages is different, both forms retain the hindered disulfide with *gem*-dimethyl substitution, thus offering an additional method for drug release through disulfide cleavage. In general, these conjugation methods provide conjugates with loadings of an average of two to three molecules of calicheamicin per antibody.

Anti-MUC1 conjugates<sup>[86,87]</sup> with the IgG1 antibody CTM01 linked to calicheamicin using the two different linkages were evaluated in vitro, and both conjugates were potent and specific in a one-hour-exposure assay. However, the carbohydrate conjugate lost virtually all specificity in a continuous-exposure assay (4 days), probably because of extracellular hydrolytic cleavage of the less stable hydrazone bond to release calicheamicin. This lack of in vitro specificity is consistent with the slightly increased toxicity of the hydrazone-linked conjugate over that of the amide-linked conjugate. In vivo, the amide conjugate was also found to be at least as active as the hydrazone conjugate against a number of different tumor models, while showing enhanced activity against tumors overexpressing PgP multidrug resistance. This data seems to suggest, at least within the context of this anti-MUC1 conjugate, that the hindered disulfide of the amide conjugate allows sufficient release of intracellular calicheamicin through glutathione reduction. In light of this data, an anti-MUC1 calicheamicin amide conjugate, CMB-401, was pursued in clinical trials against ovarian and lung cancers, however, only limited evidence of activity was observed.<sup>[87]</sup>

Calicheamicin was also linked through either a carbohydrate or amide linkage, as described above, to prepare anti-

CD33 conjugates using the murine antibody P67.6.<sup>[85,88]</sup> Interestingly, unlike for the anti-MUC1 conjugates, there was a clear preference in vitro for the acid-labile conjugate, as it was found to be almost 7000 times more potent than the corresponding amide conjugate toward antigen-positive HL-60 cells. These results suggest a different mechanism of cellular processing for the two targets. The P67.6 amide conjugates, while active, did not produce long-term durable responses upon in vivo evaluation in xenograft models, whereas the carbohydrate conjugate was found to eradicate most tumors (9/10) at doses of both 150 and 300  $\mu\text{g kg}^{-1} \times 3$ . In light of these contrasting results between antibody (anti-MUC1 versus anti-CD33) and linkage type, it is apparent that a single conjugate-linkage design is not necessarily optimal for all antibody conjugates.

While the process of oxidizing the murine form of the P67.6 antibody with sodium periodate had been successful in preparing hydrazone-linked calicheamicin conjugates, similar attempts with a humanized form of the antibody were accompanied by a loss in binding affinity and drug loading.<sup>[88]</sup> Thus, the conjugate was redesigned with the goal of preserving the hydrazone link but conjugating through the lysine residues of the antibody, thus avoiding the need for antibody oxidation. From a set of 36 different hybrid linkers (representative set shown in Figure 26) that were evaluated,<sup>[88]</sup> the AcBut linker (linker B) was chosen, as it showed good stability at pH 7.4 (94%) and almost complete hydrolysis at pH 4.5 (97%) at 37°C for 24 hours, thus indicating that this

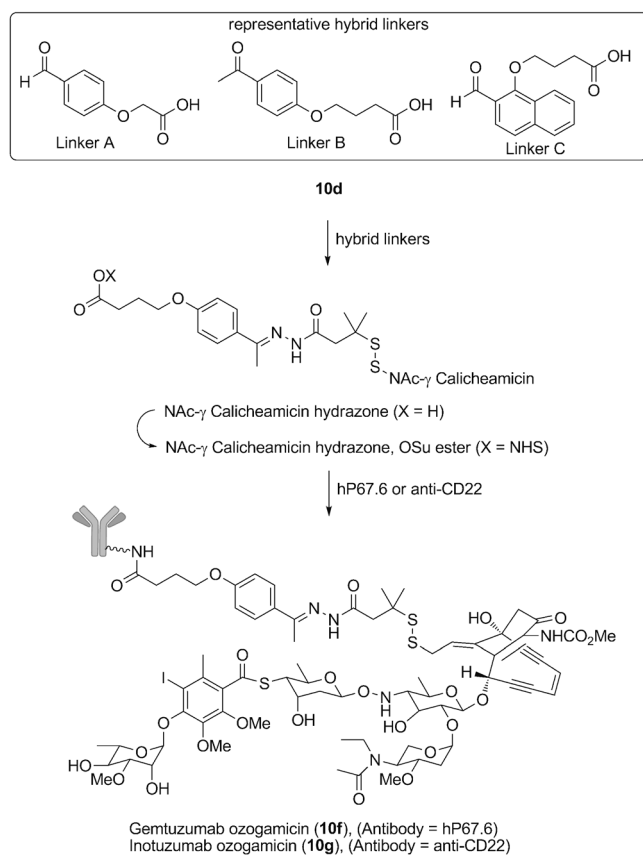


Figure 26. Synthesis of ADCs with calicheamicin.

linker should have good stability during circulation in blood plasma, yet be readily cleaved once in the acidic lysosomes. The hP67.6-NAc-γ calicheamicin DMH AcBut conjugate (10f) was found to be very potent toward antigen-positive HL-60 cells and over 100000 times more potent than the nontargeting MOPC-21 conjugate, thus indicating high conjugate selectivity. In vivo, the conjugate was found to induce complete tumor regressions in HL-60 tumor xenografts. In addition, ex vivo experiments indicated moderate inhibition of colony formation in a variety of leukemic marrow specimens from AML (acute myeloid leukemia) patients. In light of these data, 10f (CMA-676, gemtuzumab ozogamicin) was advanced to human clinical trials.<sup>[88]</sup>

CMC-544 (10g) is a second NAc-γ calicheamicin–DMH conjugate, which was prepared in a similar manner through the utilization of the AcBut hydrazone linker.<sup>[89]</sup> CMC-544 is a humanized IgG4 antibody calicheamicin conjugate that targets CD22, which is expressed on a majority of B-cell malignancies. CMC-544 was found to be stable, highly potent, and specific in vitro, and active in vivo, producing complete tumor regression in mice that bear human lymphoma xenografts, with animals reported to be tumor-free for more than 100 days.<sup>[90]</sup> Currently, 10g (inotuzumab ozogamicin) is being evaluated in numerous clinical trials, including a phase III trial in acute lymphoblastic leukemia (ALL).<sup>[91]</sup>

## 6.2. (+)-CC-1065 and the Duocarmycins as ADC Payloads

The duocarmycins, such as duocarmycin A (11a) and SA (11b; Figure 27), are a family of naturally occurring anti-bacterial agents initially isolated in the late 1970s from the bacterial cultures of *Streptomyces zelensis*.<sup>[92]</sup> The chemical structure of (+)-CC-1065 (4a), a member of the duocarmycin family, was confirmed in 1980 and shown to include a series of three connected pyrroloindole subunits with one of them containing an unprecedented spirocyclic cyclopropapyrrolo-

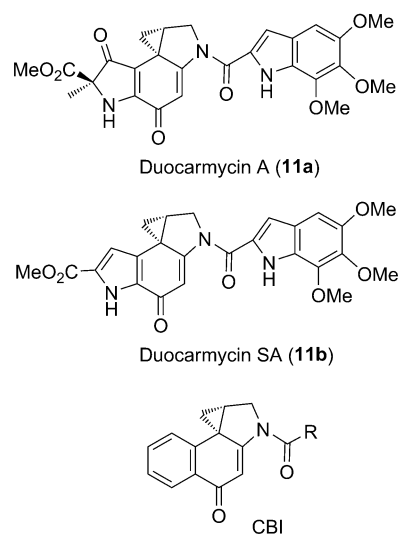


Figure 27. Structures of duocarmycins A and SA, and the cyclopropa-benzindole (CBI) moiety.



indole (CPI) moiety.<sup>[93]</sup> At the time of its discovery, **4a** was among the most potent antitumor antibiotics known.<sup>[94]</sup> The duocarmycins, and **4a** in particular, exert their high potency through a sequence-specific alkylation of DNA, preferring a five-base-pair AT-rich sequence that better accommodates the central pyrroloindole subunit. Thus, within the minor groove of DNA, the N3 of adenine attacks the cyclopropane moiety at the least substituted carbon atom of **4a**, as shown in Figure 28, thus forming a DNA adduct. The DNA alkylation ultimately results in cell death.<sup>[95]</sup>

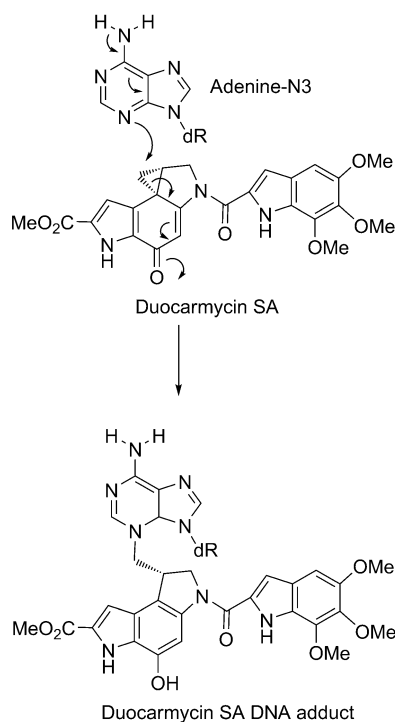


Figure 28. Mechanism of DNA alkylation for duocarmycin SA.

Clinical development of **4a** was not pursued, as it was shown to produce delayed toxicity in mice. The effort to circumvent this problem eventually led to the synthesis of molecules such as adozelesin (**4b**), carzelesin (**4c**), and bizelesin (**4d**; Figure 3). While these molecules circumvented the associated concerns regarding delayed toxicity, they were all found to possess only limited therapeutic activity in the clinic.<sup>[96,97]</sup> However, the resulting lessons learned through these efforts led to a better understanding of the structure of duocarmycins and provided insight that was useful for the development of the duocarmycins as ADC payloads. For instance, the use of a chloromethyl substituent as a precursor to the reactive cyclopropyl group only slightly decreased in vitro and in vivo activity, thus indicating that ring closure, either chemically or enzymatically, occurred quickly (Figure 29).<sup>[96,98]</sup> As a result, the CPI moiety could be derivatized in its ring open chloromethyl form in the phenolic state, which allowed the preparation of various types of prodrugs, such as carbamoyl, glycosyl, peptidyl, and carbon-

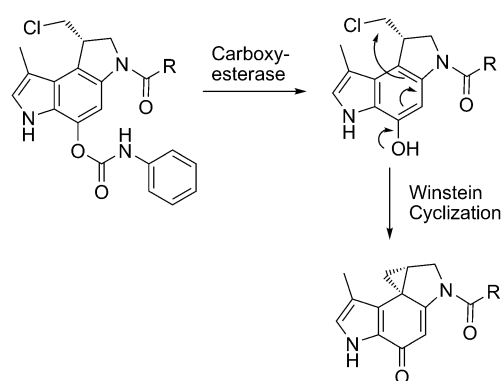


Figure 29. Mechanism for the conversion of carzelesin to its activated form through the Winstein cyclization.

ate derivatives. The incorporation of such a prodrug functional group could help to control the rate of formation of the DNA-reactive cyclopropyl group, improve the overall chemical stability, and increase the water solubility. Finally, Boger and co-workers described the synthesis of a synthetically more accessible cyclopropabenzindole (CBI, Figure 27) as a way to replace the alkylating CPI subunit, thus resulting in compounds that were still potent, but about four times more stable.<sup>[99–101]</sup>

Efforts to utilize these findings were initially realized in the synthesis of the analogue DC1, which incorporated the more stable chloromethyl surrogate, the CBI alkylating subunit, and a thiol-containing linker incorporated into the terminal pyrroloindole subunit for conjugation to an antibody (Figure 30).<sup>[102]</sup> Antibody-DC1 conjugates that contained about three to four DC1 molecules per antibody and were linked by disulfide bonds, were prepared and shown to be highly cytotoxic with  $IC_{50}$  values in the low picomolar range, and with a greater than 1000-fold selectivity for antigen-positive cells. While the lead conjugate, anti-B4-DC1, was active in human tumor xenograft models, its poor solubility and instability in the aqueous buffered solution precluded further development.

In order to circumvent these issues, analogues of DC1 were prepared in which a phosphate prodrug was incorporated into the phenol group of the CBI subunit. This incorporation resulted in compounds (DC4 and DC44; Figure 30) with significantly better solubility (3000 times better than DC1) under the required aqueous conjugation conditions, and greatly improved aqueous stability.<sup>[103]</sup> Incorporation of the phosphate prodrug did not alter the in vitro potency or specificity of the huB4-DC conjugates, thus indicating that cancer cells possessed the needed phosphatases to activate the prodrug intracellularly.<sup>[103]</sup>

Additional efforts to expand upon the information gained from duocarmycin research can be found in the ADC MDX-1203. This conjugate contains a synthetic duocarmycin derivative that is conjugated to a human anti-CD70 antibody (Figure 30). The duocarmycin analogue incorporates the chloromethyl surrogate, a piperazino carbamate prodrug at the phenol moiety of the CBI unit, and a modified terminal pyrroloindole subunit that bears a substituted aniline. The

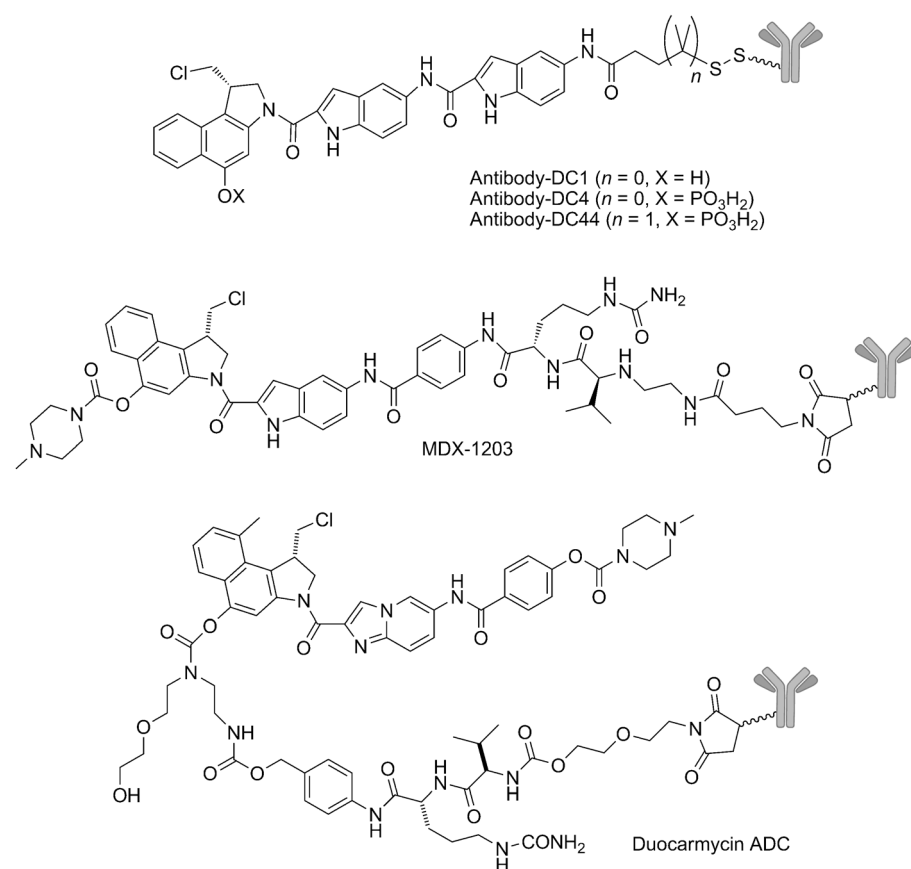


Figure 30. Structures of second-generation duocarmycin ADCs.

substituted aniline allows linkage to the antibody by a linker containing a valine–citrulline dipeptide (val–cit). Once the conjugate is internalized, the dipeptide is cleaved, thus releasing the aniline-bearing duocarmycin, which is then activated by carbamate cleavage, presumably by carboxyl esterase. MDX-1203 was shown to possess potent antigen-specific activity both in vitro and in vivo and was subsequently advanced to clinical trials against renal cell carcinoma and non-Hodgkin's lymphoma.

An alternative way to link duocarmycins is shown in Figure 30. In this case, a methyl piperazine carbamate was incorporated at the terminal pyrroloindole, while a peptide-containing linker was connected through the phenol moiety of the CBI unit.<sup>[104]</sup> The linker employs a cleavable peptide, which releases a *p*-amino benzyl group that undergoes a series of self-immolations, ultimately releasing the active duocarmycin. These conjugates have been linked to trastuzumab by thiol groups, which were generated through the reduction of interstrand cystines of the antibody, thus providing conjugates with an average of two duocarmycins linked per antibody. Modulation of the linker length was shown to effect conjugate stability in human plasma, and the conjugates were found to be potent in vitro. In vivo antitumor activity was shown to depend on the length of the linker and choice of drug.

### 6.3. SN-38 and the Camptothecins

Camptothecin (CPT, **12a**), a pentacyclic quinolone-based plant alkaloid, was first isolated from the deciduous Asian tree *Camptotheca acuminata* in 1966 by Wani and Wall (Figure 31).<sup>[105]</sup> CPT was shown to possess potent antitumor activity by selectively inhibiting DNA topoisomerase I, thus effectively stalling DNA replication in S-phase arrest and resulting in the apoptotic cell death of tumor cells.<sup>[106]</sup> Like the duocarmycins, **12a** suffered from drawbacks that prevented its clinical development, such as poor water solubility and the ease of physiological conversion of the lactone to its inactive ring-opened carboxylate form. Research that aimed at improving these attributes led to the development of topotecan (**12b**) and irinotecan (**12c**), which have been approved by the FDA as anticancer drugs.<sup>[107,108]</sup> While the conversion to a water-soluble piperazine pro-drug form, as in **12c**, was sufficient to render it clinically effective, it did so with reduced potency as a result of inefficient carboxyl-

esterase-catalyzed hydrolysis of the prodrug to its active metabolite, SN-38 (**12d**), in patients.

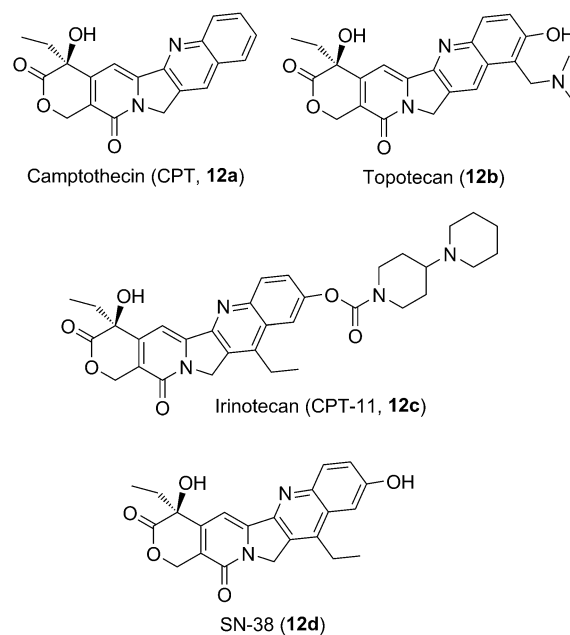
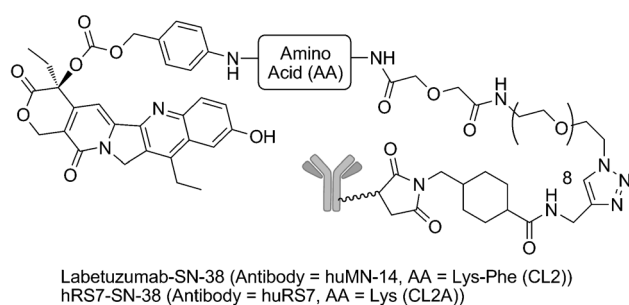


Figure 31. Chemical structures of camptothecin (CPT) and its clinically relevant analogues.

In an effort to conjugate **12d** to an antibody, linkage of the molecule through its hydroxy group at C20 has been evaluated.<sup>[109–114]</sup> This approach effectively serves the dual purpose of a) providing a handle for linker incorporation, and b) helping to minimize lactone ring opening under physiological conditions. Current efforts have focused on the use of either the CL2 linker, which contains a solubilizing spacer connected to a pH-sensitive *p*-aminobenzyl carbonate by a lysine-phenylalanine dipeptide,<sup>[109]</sup> or the CL2A linker, which possesses a single lysine residue.<sup>[110,111]</sup> Using these linkers, **12d** was conjugated to cysteine residues, obtained through reduction of the antibody, by thioether bonds to give conjugates with an average of about six molecules of SN-38 per antibody. These conjugates have been shown to be somewhat unstable in human serum, thus releasing about 50% of the active metabolite **12a** per day.<sup>[112]</sup> However, because of the targeting nature of the antibody, the majority of metabolite is released locally at the tumor and it has been suggested that internalization may not be required for activity.<sup>[110]</sup>

The clinically most advanced SN-38 conjugate, labetuzumab-SN-38 (Figure 32), consists of the humanized hMN-14 antibody, which targets carcinoembryonic antigen (CD66e),



**Figure 32.** Structures of labetuzumab-SN-38 and hRS7-SN-38 ADCs.

linked to **12d** using the CL2 type linker. In preclinical studies, labetuzumab-SN-38 (IMMU-130) was shown to significantly extend the median survival time of nude mice that bear a variety of different human colorectal and pancreatic carcinomas, compared to both non-targeting controls and CPT-11.<sup>[113]</sup> Currently, IMMU-130 is being evaluated in two different Phase I clinical trials for patients with relapsed/refractory colorectal cancers. hRS7-SN-38 (IMMU-132) is a conjugate of **12a** connected by the CL2A linker with the humanized Trop-2 antibody, which targets the human trophoblast cell-surface antigen expressed on a variety of human carcinomas, including many epithelial cancers. Preclinical studies with IMMU-132 demonstrated antitumor effects superior to nontargeting controls at nontoxic doses in mice that bear a variety of different tumor types.<sup>[114]</sup> Currently, IMMU-132 is in a Phase I study for patients with advanced epithelial cancers. Preclinical work for SN38 conjugates directed to two other target antigens, milatuzumab-SN-38<sup>[112]</sup> and epratuzumab-SN-38,<sup>[110]</sup> has also been described.

## 7. Clinical Results

The first ADC to gain marketing approval from the U.S. FDA was gemtuzumab ozogamicin (**10f**; Figure 26), which consists of the highly cytotoxic DNA-strand-breaking calicheamicin compound linked by a hydrazone linker to a CD33 antibody. Its accelerated approval in 2000 was based on single-arm Phase II clinical trials, and was indicated for the treatment of patients who were 60 years and older in first relapse with CD33+ AML and who were not considered candidates for chemotherapy.<sup>[115]</sup> Subsequently, gemtuzumab ozogamicin was withdrawn from the market in 2010, when a confirmatory clinical trial, in combination with chemotherapy, raised toxicity concerns and did not show sufficient clinical benefit (improvement in survival time).<sup>[116,117]</sup> Recent reports from other studies suggest that the ADC may well provide clinical benefit with modified dosing regimens.<sup>[117]</sup>

Currently, two ADCs are approved for cancer therapy: CD30-targeting brentuximab vedotin for use in Hodgkin lymphoma and anaplastic large cell lymphoma (ALCL), and HER2-targeting ado-trastuzumab emtansine (T-DM1) for use in metastatic breast cancer (Figure 33). The two ADCs employ different microtubule-disrupting agents as the payload.

Brentuximab vedotin consists of monomethyl auristatin E (MMAE), a synthetic analogue of dolastatin-10, linked to the chimeric CD30 antibody cAC10 at cysteine residues by a valine-citrulline dipeptide linker that contain a *p*-aminobenzylcarbamate (PABC) self-immolative spacer. The valine-citrulline dipeptide is designed to be cleaved in lysosomes (by cathepsin B), leading to self-immolation of the PABC moiety and release of MMAE.<sup>[74,118]</sup> The unconjugated anti-CD30 antibody cAC10 was previously tested in the clinic, but did not show sufficient activity as a single agent to progress beyond phase I and II clinical trials (8% overall response rate).<sup>[119]</sup> In contrast, the compelling clinical activity of its MMAE conjugate, brentuximab vedotin, led to accelerated approval by the FDA in 2011.<sup>[120,121]</sup> In a pivotal phase II trial in relapsed or refractory Hodgkin lymphoma, brentuximab vedotin given at 1.8 mg kg<sup>-1</sup> every three weeks showed an overall response rate (ORR) of 75%, with 34% and 40% of patients achieving complete response (CR) and partial response (PR), respectively. In relapsed or refractory systemic ALCL, the ORR was 86%, with CR in 53% of patients.<sup>[120,122]</sup>

The first approved ADC for the treatment of solid tumors, ado-trastuzumab emtansine, is a conjugate of the anti-HER2-antibody trastuzumab linked at lysine residues with the maytansinoid DM1 by the noncleavable SMCC thioether linker. Release of the active species, the lysine-linked maytansinoid, occurs once the ADC is internalized and routed to lysosomes, where the antibody moiety is completely degraded to its constituent amino acids. Intracellular release of the lysine-linked maytansinoid leads to cell-cycle arrest and ultimately to target cell death.<sup>[65]</sup> The safety and effectiveness of ado-trastuzumab emtansine was evaluated in a Phase III clinical study in 991 patients randomly assigned to receive ado-trastuzumab emtansine at 3.6 mg kg<sup>-1</sup> every three weeks, or an established regimen of lapatinib plus capecitabine. In

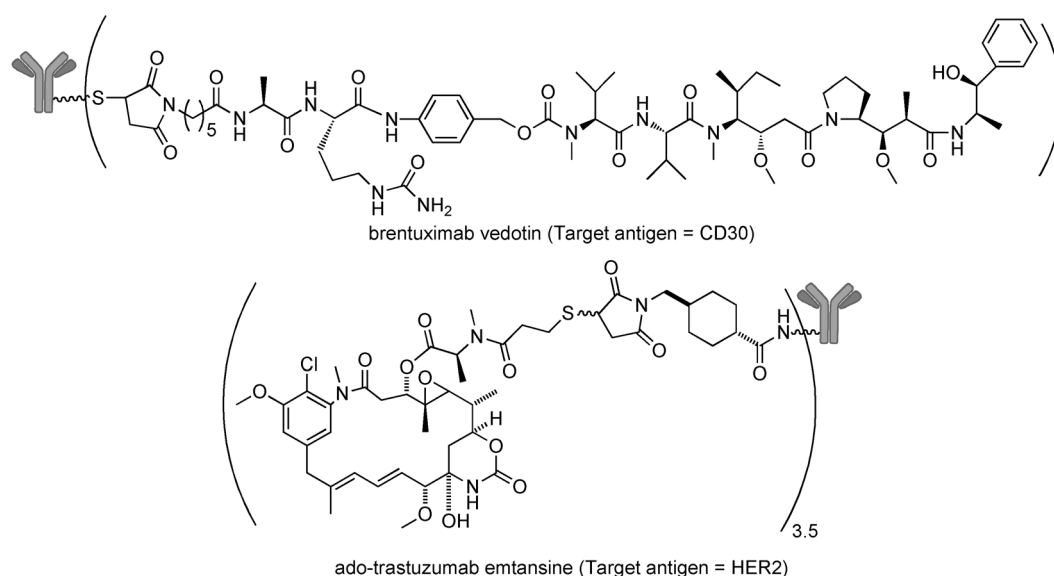


**Figure 33.** Structures of brentuximab vedotin and ado-trastuzumab emtansine.

these HER2+ metastatic breast cancer patients who had previously been treated with trastuzumab plus a taxane, ado-trastuzumab emtansine showed an improved median progression-free survival of 9.6 months and median overall survival of 30.9 months, versus median progression-free survival (PFS) of 6.4 months and median overall survival of 25.1 months for the combination of lapatinib plus capecitabine. Ado-trastuzumab emtansine also demonstrated a favorable safety profile compared to that of the chemotherapeutic combination of lapatinib and capecitabine.<sup>[123]</sup> These data led to ado-trastuzumab emtansine receiving full marketing approval by the FDA in 2013<sup>[123,124]</sup> for treatment of HER2+ positive metastatic breast cancer patients who had previously received trastuzumab and a taxane, the first ADC to receive such full approval.

A number of ADCs are in various stages of clinical evaluation (Table 3). A majority of them employ microtubule-disrupting compounds (maytansinoids or auristatins) as the payload. The two approved ADCs ado-trastuzumab emtansine and brentuximab vedotin are undergoing additional clinical trials to broaden the treatment indications. For example, in a phase II trial, patients ( $N=137$ ) with HER2-positive metastatic breast cancer or recurrent locally advanced breast cancer were randomly assigned to trastuzumab plus docetaxel ( $n=70$ ) or T-DM1 ( $n=67$ ) as first-line treatment. The T-DM1 arm showed an overall response rate of 69.2% compared to 58.0% for the comparator arm. T-DM1 also showed a significantly improved PFS compared to the trastuzumab plus docetaxel (14.2 months versus 9.2 months). Furthermore, T-DM1 had a favorable safety profile over standard first-line treatment with fewer grade  $\geq 3$  adverse events (46.4% versus 90.9%).<sup>[125]</sup> Based on these promising results, a randomized Phase III clinical trial is ongoing.

Brentuximab vedotin is being tested in three different Phase III trials, including front line treatment in combination with chemotherapy in Hodgkins lymphoma and CD30+

mature T-cell lymphoma. The ADC, inotuzumab ozogamicin (**10g**; Figure 26), which consists of an anti-CD22 antibody linked to NAc- $\gamma$  calicheamicin via a hydrazone linker, is currently undergoing a Phase III study in CD22+ adult ALL.<sup>[126]</sup> This ADC was recently withdrawn from a Phase III study in CD22+ non-Hodgkin lymphoma because of a lack of improvement in overall survival.

## 8. Emerging Technologies

### 8.1. New Effector Molecules

#### 8.1.1. Benzodiazepine Dimers

The pyrrolobenzodiazepine (PBD) class of molecules was first discovered in the 1960s, when anthramycin (**13a**) was isolated as the active constituent from the fermentation broth of *Streptomyces refuineus* var. *thermotolerans*.<sup>[127,128]</sup> As a result of its promising antibiotic and antitumor activity, the search for additional PBDs led to the discovery of 13 different natural PBD monomer types and a diverse range of synthetic analogues (Figure 34).<sup>[129]</sup> These PBD monomers are differentiated in the substitution patterns that are present in their A and C rings and the saturation level of the C ring, with an increased unsaturation typically rendering the PBD monomers biologically more active. Mechanistically, the PBDs exert their biological activity through their ability to react through the N10–C11 imine/carbinolamine functionality with the amino group in C2 position of a guanine residue within the minor groove of DNA, as shown in Figure 35.

PBD monomers were shown to prefer a three-base-pair sequence in which the guanine residue was flanked by purines on both sides. As a result of this, Thurston and co-workers sought to further explore this sequence selectivity in the form of PBD dimers that would form irreparable DNA cross-links.<sup>[130]</sup> A PBD dimer, DSB-120 (**13e**), was prepared by linking two molecules of the natural product DC-81 (**13d**) by



**Table 3:** List of antibody–drug conjugates currently in clinical trials.

Candidate	Drug	Antigen	Lead Indication <sup>[a]</sup>	Developer/Partner
<b>FDA-Approved</b>				
ado-Trastuzumab emtansine (Kadcyla)	DM1	HER2	Breast Cancer	Roche/Genentech/ImmunoGen
Brentuximab vedotin (Adcetris)	MMAE	CD30	HL/ALCL	Seattle Genetics
<b>Phase III</b>				
Inotuzumab ozogamicin (CMC-544)	Calicheamicin	CD22	ALL	Pfizer
Gemtuzumab ozogamicin (CMA-676)	Calicheamicin	CD33	AML	Pfizer
<b>Phase II</b>				
SAR3419	DM4	CD19	B-Cell malignancies	Sanofi/ImmunoGen
RG7593	MMAE	CD22	B-Cell malignancies	Roche/Genentech/Seattle Genetics
RG7596	MMAE	CD79b	B-Cell malignancies	Roche/Genentech/Seattle Genetics
Glembatumumab vedotin (CDX-011)	MMAE	GPNUMB	Breast Cancer, Melanoma	Celldex Therapeutics/Seattle Genetics
PSMA-ADC	MMAE	PSMA	Prostate Cancer	Progenics Pharma/Seattle Genetics
<b>Phase I</b>				
Lorvotuzumab mertanisine	DM1	CD56	SCLC	ImmunoGen
IMGN529	DM1	CD37	B-Cell malignancies	ImmunoGen
IMGN853	DM4	FR $\alpha$	Solid Tumors	ImmunoGen
IMGN289	DM1	EGFR	Solid Tumors	ImmunoGen
SAR56658	DM4	CA6	Solid Tumors	Sanofi/ImmunoGen
BT-062	DM4	CD138	Multiple Myeloma	Biotest/ImmunoGen
BAY 94-9343	DM4	mesothelin	Solid Tumors	Bayer/ImmunoGen
AMG 595	DM1	EGFRvIII	Gliomas	Amgen/ImmunoGen
AMG 172	DM1	CD27L	ccRCC	Amgen/ImmunoGen
SGN-CD19A	MMAF	CD19	NHL/ALL	Seattle Genetics
AGS-22ME	MMAE	Nectin 4	Solid Tumors	Astellas Pharma/Seattle Genetics
RG7450	MMAE	STEAP1	Prostate Cancer	Roche/Genentech/Seattle Genetics
RG7458	MMAE	MUC16	Ovarian Cancer	Roche/Genentech/Seattle Genetics
RG7599	MMAE	NaPi2b	NSCLC, Ovarian Cancer	Roche/Genentech/Seattle Genetics
MLN0264	MMAE	GCC	GI Malignancies	Takeda/Seattle Genetics
SGN-CD33A	PBD	CD33	AML	Seattle Genetics
MDX-1203	Duocarmycin	CD70	NHL, RCC	Bristol-Myers Squibb
Labetuzumab-SN-38	SN-38	CD66e	CRC	Immunomedics
IMMU-132	SN-38	Trop-2	Epithelial Cancers	Immunomedics
Milatuzumab Doxorubicin	Doxorubicin	CD74	Multiple Myeloma	Immunomedics
RG7598, RG7600, RG7636	Undisclosed	Undisclosed	Various	Roche/Genentech/Seattle Genetics

[a] HL: Hodgkin's Lymphoma; ALCL: Anaplastic Large Cell Lymphoma; NHL: Non-Hodgkin's Lymphoma; AML: Acute Myelogenous Leukemia; SCLC: Small-Cell Lung Cancer; ccRCC: Clear Cell Renal Cell Carcinoma; RCC: Renal Cell Carcinoma; ALL: Acute Lymphoblastic Leukemia; NSCLC: Non-Small-Cell Lung Cancer; GI: Gastrointestinal; CRC: Colorectal Carcinoma.

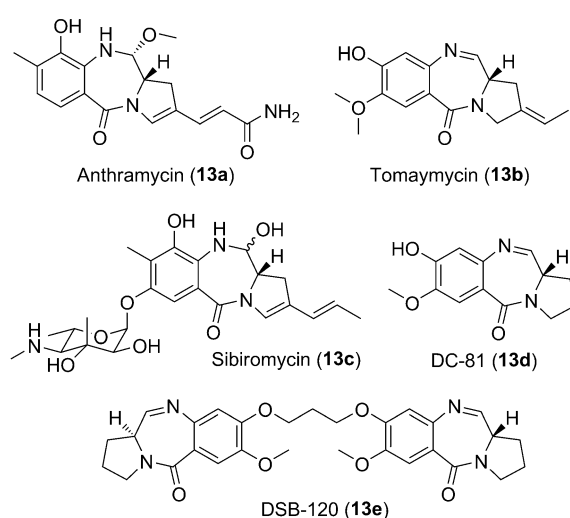


**Figure 34.** Pyrrolobenzodiazepine (PBD) monomers and DSB-120.

a propyldioxy ether linkage. Dimer formation resulted in significant increase in potency, with **13e** being 600 times more cytotoxic than **13d** in vitro. DSB-120 was shown to form DNA cross-links that spanned six base pairs with a preference for a central GATC sequence. At the time of its discovery it was among the most efficient DNA cross-linking agents known. Further elaboration of the PBD dimers eventually led to the synthesis of SJG-136 (**4f**; Figure 3) in which additional unsaturation was incorporated into the C rings of **13e**.<sup>[131,132]</sup> As a result, **4f** was shown to demonstrate significantly better DNA cross-linking efficiency and exquisite in vitro potency and good in vivo antitumor activity.<sup>[133]</sup> Currently, SJG-136 is being evaluated in Phase II clinical studies against solid tumors and hematologic malignancies.<sup>[134]</sup>

Because of their high potency and DNA-interacting mechanism of action, the PBD dimers are attractive effector molecules for use in ADCs. In 2009, a new class of potent compounds (IGNs) was described, consisting of two indolino-benzodiazepine monomers linked by an anilino-benzylidenoxy

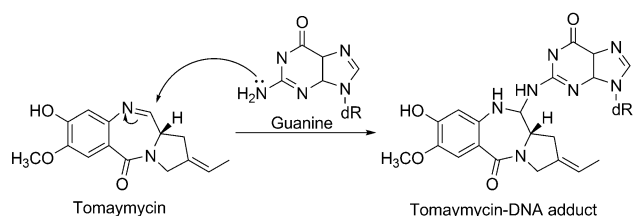


**Figure 35.** Mechanism of action of pyrrolobenzodiazepine (PBD).

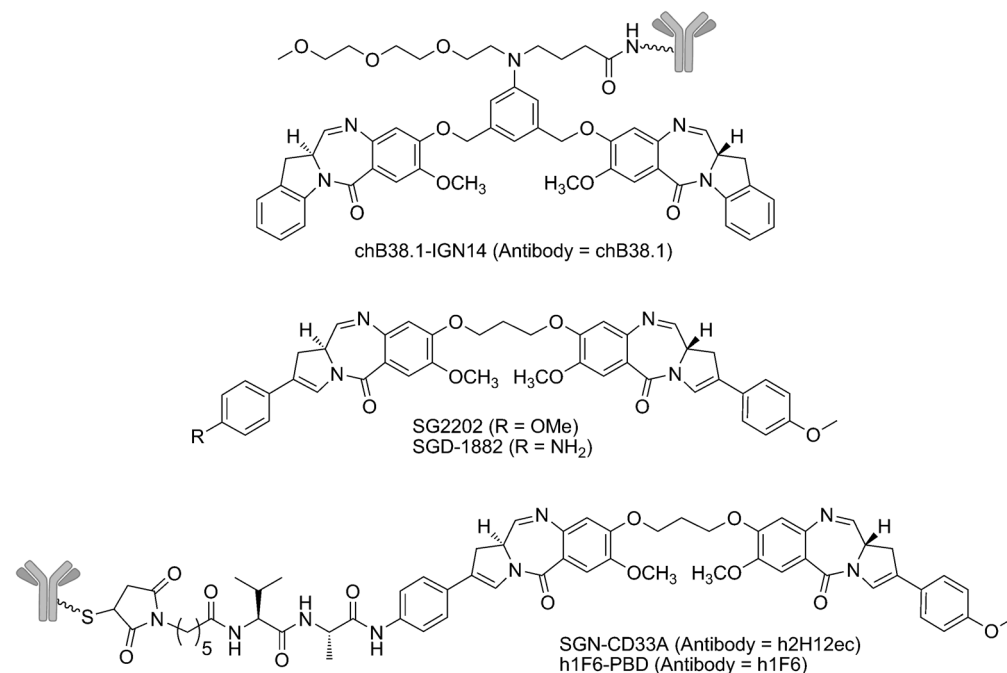


**Figure 36.** Indolinobenzodiazepine (IGN) and pyrrolobenzodiazepine (PBD) dimer conjugates.

spacer (Figure 36).<sup>[135]</sup> The parent compound of this class displayed potent sequence-specific DNA–adduct formation in double-stranded DNA and was extremely potent (1–10  $\mu\text{M}$ ) against a variety of cancer cell types. The incorporation of the anilino group into the spacer results in a suitable site for the incorporation of a linker for conjugation to an antibody. Incorporation of a short PEG group provided the necessary solubility in water for conjugation in aqueous media. ADCs of these IGNs containing an average of three molecules linked per antibody were prepared and found to be highly potent in vitro against both normal and multi-drug-resistant cancer cell lines ( $\text{IC}_{50}$  = 5–20  $\mu\text{M}$ ). Even cell lines that express low levels of antigen ( $\approx 7000$  molecules per cell) were efficiently killed by the conjugate ( $\text{IC}_{50}$  value of 4  $\mu\text{M}$ ). In addition, the cytotoxic effect of the conjugate was found to be antigen-specific, as the conjugate was considerably less cytotoxic to an antigen-negative cell line ( $\text{IC}_{50}$  > 1  $\mu\text{M}$ ). Dose-dependent antigen-specific antitumor activity in vivo was also reported.

Recently, two ADCs that utilize the PBD dimer SG2202,<sup>[134]</sup> which possesses an exocyclic phenyl substituent attached to the C ring (Figure 36), were described.<sup>[136,137]</sup> The incorporation of styryl groups was found to further increase

the in vitro potency of the PBD dimer, while also providing the opportunity to introduce substituents for linking the PBD dimer to an antibody. In the ADC design, one of the monomer units is modified with an anilino substituent, thus generating an unsymmetrical PBD dimer, which was then modified with a valine-alanine dipeptide connected to a maleimide. Conjugates containing 1.9 PBD molecules per antibody were then prepared by linkage through engineered cysteine residues introduced into the antibody sequence.<sup>[136,137]</sup>

ADCs that target the CD70 antigen, expressed on renal cell carcinoma (RCC) and non-Hodgkin lymphoma (NHL), and the CD33 antigen, expressed in acute myeloid leukemia (AML), were found to be potent and specific on a number of antigen-expressing cell lines in vitro. In vivo, both ADCs displayed dose-dependent antitumor activity in xenograft models in mice. In light of these data, an anti-CD33-PBD conjugate has recently been advanced to clinical evaluation in AML.<sup>[137]</sup>

### 8.1.2. Amanitin

The amanitins are mushroom toxins derived from the genus *Amanita*.

The main component,  $\alpha$ -amanitin, is a bicyclic octapeptide that has been shown to be a potent RNA polymerase II inhibitor.  $\alpha$ -Amanitin is not therapeutically useful as it is efficiently transported to mature hepatocytes in vivo where it causes high liver toxicity.  $\alpha$ -Amanitin has been linked to trastuzumab, and the conjugate displays antigen-specific potency toward HER2+ cell lines ( $\text{IC}_{50}$ : 8–180  $\mu\text{M}$ ).<sup>[138]</sup> In vivo, complete tumor regressions were obtained at low doses (0.05  $\text{mg kg}^{-1}$  linked amanitin) and liver toxicity was not noted at the tested doses. Information about the MTD and therapeutic index of this conjugate were not reported.

### 8.2. Site-Specific-Conjugation Technology

ADCs that are currently in clinical evaluation take advantage of functional groups (primary amino group of lysines, thiol groups from reduction of cystines) in antibodies that are amenable to chemistry in aqueous solutions. A humanized antibody contains a large number of lysine groups (80–90), therefore allowing the modification of a few lysine groups without affecting the native disulfide bonds and

without causing any significant changes in the stability and biophysical or binding properties of the antibody. Mass spectral analysis of a maytansinoid ADC, with an average load of 3.5–4 molecules per antibody, shows a distribution of peaks corresponding to a range of 0–7 maytansinoid molecules per antibody, which approximately fits a binomial distribution.<sup>[139]</sup> The lysine sites of maytansinoid attachment are consistent from batch to batch under controlled conjugation conditions. Antibody–lysine site modification is used for ado-trastuzumab emtansine, as well as for all other maytansinoid conjugates currently undergoing clinical evaluation. Antibody–lysine site modification is also employed for calicheamicin conjugates.

The cysteine conjugation site used in ADCs is generated by reducing native interchain cystine disulfide bonds, and the drug load is determined by the extent of the reduction. Typically, a fully reduced IgG<sub>1</sub> antibody has about eight cysteine residues. Partial disulfide reduction and loading of about four molecules of a cytotoxic agent per antibody at the cysteine sites also leads to a distribution of several species with 0, 2, 4, 6, and 8 molecules of the cytotoxic agent attached, with species with a load of 4 and 2 molecules being predominant.<sup>[140,141]</sup> Brentuximab vedotin and other auristatin-based ADCs are conjugated by cysteines that were generated by such partial reduction of native interchain disulfide bonds. An advantage of lysine or reduced-disulfide cysteine sites for the attachment of cytotoxic agents is that any antibody can be conjugated without re-engineering the antibody to introduce specific sites of attachment.

In order to increase the drug load in the ADC, one recently reported approach involves the use of a dendrimeric carrier for the drug. The basis of this method is the use of a hydrophilic, fully degradable polyacetal carrier that bears two orthogonal linkers. One linker was used to connect the carrier to an antibody by cysteine residues, derived from reduction of native cystine bridges in the hinge region of the antibody. The second linker was used to conjugate a dolastatin analogue. A conjugate of trastuzumab with 3–4 polyacetal carriers bearing a total of 20 dolastatin molecules was shown to display good antigen-specific potency in vitro and significant antitumor activity in vivo.<sup>[142]</sup>

Several approaches are currently evaluated to effect “site-specific” conjugation where sites of attachment of the cytotoxic agent to the antibody are defined. In addition, this approach is expected to give a single ADC species instead of a distribution. In the first described approach, cysteine residues were engineered in antibodies, for example by replacing serine 442 with cysteine in the CH3 domain of the heavy chain, resulting in the generation of two thiol groups per antibody.<sup>[143]</sup> Antibodies that did not interfere with antigen binding (“thiomabs”) and contained engineered cysteines at various positions were conjugated with maleimido-MMAE to give homogeneous ADCs with two linked MMAEs per antibody. The site of cysteine incorporation was important, because thiol-maleimide linkages that were unstable in plasma were formed at some cysteine sites.<sup>[139,144]</sup> A homogeneously conjugated anti-MUC16 conjugate with two MMAEs per antibody (one per heavy chain), linked by an engineered cysteine in each heavy chain, showed similar

efficacy in xenograft models and improved tolerability in rat and monkey preclinical models compared to a conjugate with an average of 3.1 MMAEs per antibody, derived from reduced interchain disulfide conjugation.<sup>[141]</sup> Cysteine-engineered antibodies require additional manufacturing steps compared to traditional antibodies because of their initial generation from cell culture as mixed disulfides, which require partial reduction and reoxidation.<sup>[141]</sup> One ADC derived from an engineered cysteine antibody has recently entered into clinical evaluation.<sup>[137]</sup>

Four other approaches to generate site-specific ADCs through antibody engineering and other techniques are underway. These include: a) The incorporation of an unnatural amino acid through genetic engineering.<sup>[145]</sup> In this elegant approach, the appropriate tRNA/aminoacyl-tRNA synthetase pair was used to replace an alanine residue in the heavy chain of the trastuzumab antibody with the unnatural amino acid *para*-acetylphenylalanine. The incorporation of an amino acid with a carbonyl moiety, a functional group that is not present in any of the 20 natural amino acids, provides orthogonal chemical reactivity. The antibody mutant was conjugated to an auristatin derivative through a stable oxime link to provide a homogenous ADC with two molecules of drug linked in a site-specific manner (Figure 37). The resulting conjugate displayed good in vitro potency and in vivo antitumor activity, along with favorable pharmacokinetics. b) The incorporation of engineered glutamine residues and coupling of amino groups of the cytotoxic agent by amide linkage using microbial transglutaminase (mTG).<sup>[146]</sup> This approach takes advantage of the finding that mTG does not recognize naturally occurring glutamine residues in the constant regions of glycosylated antibodies. Thus, glutamine residues were engineered at selected sites in three different antibodies. Treatment with mTG in the presence of an acyl acceptor payload (AcLys-vc-monomethylauristatin D) resulted in the incorporation of around two drug molecules per antibody in a site-specific manner. In one example, ADCs that bear 1.74 and 1.87 drug molecules per antibody were shown to be potent in vitro, and displayed similar in vivo antitumor activity when compared to a traditional conjugate that bears 3.6 auristatin molecules per antibody. c) The site-specific modification of heavy-chain C termini by intein fusion,<sup>[147]</sup> and d) the incorporation of engineered cysteines at the N terminus and coupling of 1,2-aminothiol to an aldehyde group of a cytotoxic agent by a thiazolidine linkage.<sup>[148]</sup> Thus far, it was possible to link about two molecules of a cytotoxic agent to an antibody using these approaches. It is not clear whether this load will be sufficient to affect cell killing when the antigen density is not very high. Higher drug loading without affecting the biochemical characteristics of the conjugate has not yet been demonstrated with any of the site-specific approaches. It is not yet known whether site-specific conjugation will actually improve the therapeutic index of ADCs in the clinic. Also, the potential immunogenicity of ADCs that bear antibodies with unnatural amino acids can only be determined through human clinical trials.

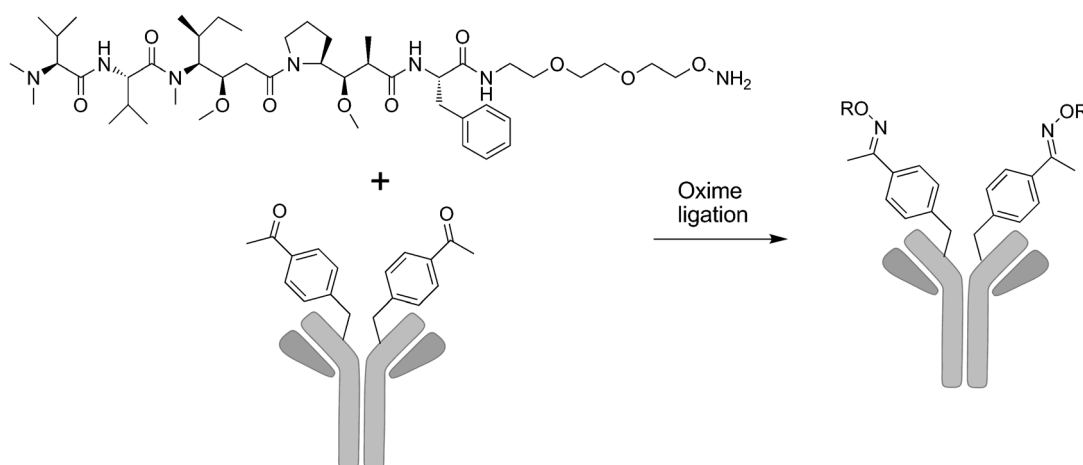


**Figure 37.** Site-specific conjugation of alkoxyamine-derivatized auristatin.

### 8.3. Optimizing ADC Activity

Further optimization of ADC design continues to be an active area of research. Use of smaller scaffold proteins or antibody fragments, instead of whole IgGs, may offer the advantage of greater tumor penetration in view of their smaller size. A direct comparison of the *in vivo* tumor localization of antibody fragments (sFv, Fab', F(ab')<sub>2</sub>) with the intact IgG showed that the rate and degree of tumor penetration correlated with the size.<sup>[149]</sup> The smallest fragment, sFv, demonstrated maximal tumor penetration at 0.5 hours, while the intact IgG took 48 to 96 hours to achieve the same level of penetration. In addition, the sFv was more evenly distributed throughout the tumor mass as compared to the forms with higher molecular weights. Despite the availability of this data for over twenty years, drug conjugates of antibody fragments have not advanced beyond the preclinical stage. The faster clearance of these fragments and the propensity to accumulate in kidneys requires half-life extension strategies, such as conjugation to poly(ethylene glycol)s, thus making the technology more complex. In one study, a diabody–auristatin conjugate was shown to clear around 30 times faster than the corresponding IgG conjugate, and was four times less potent *in vitro* and *in vivo*.<sup>[150]</sup>

Other considerations for successful ADC development include greater attention to the selection of antibodies and linkers, and more thorough preclinical evaluation prior to advancement to the clinic. It is commonly believed that antibodies have to be efficiently internalized to achieve good ADC activity. A recent report with a vascular-targeting ADC suggests that this may not always be a necessary feature.<sup>[151]</sup> The linker between the antibody and the drug determines the nature of the metabolite produced *in vitro* and *in vivo*. Recent clinical data suggests that the toxicity profile of the ADC is linker-dependent. Thus, changes in linker design would alter the metabolite profile, which in turn would influence clinical toxicity. For ADC therapy, preclinical models for efficacy studies have to be carefully selected such that the antigen expression on the xenograft reflects the clinical population to be treated. In addition, it is important to demonstrate

antitumor activity *in vivo* at doses achievable in the clinic (2–7 mg kg<sup>−1</sup> for most ADCs). Setting such higher preclinical bars may mitigate the chance of failure in the clinic.

## 9. Summary and Outlook

The concept of targeted delivery of anticancer drugs originated from the desire of oncologists to improve the tumor selectivity of anticancer drugs in order to lower their systemic toxicity. By these means, the drugs could be administered at higher doses, thus providing greater therapeutic benefit to their patients. The tumor selectivity of antibodies offered an avenue to achieve this goal by using them as vehicles to direct the drug to the tumor. This seemingly simple concept, called antibody–drug conjugates, garnered tremendous attention from researchers at academic institutions and in the pharmaceutical industry. A flurry of research and development activity in the 1980s and early 1990s led to clinical trials of several ADCs. However, disappointing clinical results led to diminishing interest in this approach.

Nevertheless, some research groups persisted and carefully analyzed the possible causes of the failures. From the lessons learned, almost every aspect of the technology was improved. The current breed of ADCs uses antibodies that are humanized, and thus not immunogenic, and linkers that are designed to be stable in circulation, but are cleaved upon delivery into a cell. Medicinal chemists are now able to harness the potency of drugs that were once too toxic to be useful on their own. The recent FDA approvals of the two ADCs, brentuximab vedotin and ado-trastuzumab emtansine, have provided proof-of-concept for this approach, and have generated tremendous excitement. There are over 30 ADCs currently in clinical evaluation and almost every major pharmaceutical company has embraced this technology. There is active research by medicinal chemists to develop new linkers and discover new potent effector molecules suitable for use in ADCs, while biologists have focused on identifying cell-surface targets suitable for antibody development.



## Acknowledgement

The early and enthusiastic support of RVJC's work on ADCs by the late Dr. Emil (Tom) Frei III, former Physician-in-Chief of the Dana-Farber Cancer Institute, is greatly appreciated. The authors sincerely thank Dr. Daniel Tavares for his creative illustrations, and Dr. John Lambert for his critical review of this manuscript and valuable comments.

Received: August 29, 2013

Published online: February 20, 2014

- [1] V. T. DeVita, Jr., E. Chu, *Cancer Res.* **2008**, *68*, 8643–8653.
- [2] B. C. Baguley in *Anticancer Drug Development* (Eds.: B. C. Baguley, D. J. Kerr), Academic Press, San Diego, **2002**, pp. 1–11.
- [3] E. Frei III, *Cancer Res.* **1972**, *32*, 2593–2607.
- [4] S. M. Kupchan, Y. Komoda, W. A. Court, G. J. Thomas, R. M. Smith, A. Karim, C. J. Gilmore, R. C. Haltiwanger, R. F. Bryan, *J. Am. Chem. Soc.* **1972**, *94*, 1354–1356.
- [5] S. M. Kupchan, Y. Komoda, A. R. Branfman, A. T. Sneden, W. A. Court, G. J. Thomas, H. P. Hintz, R. M. Smith, A. Karim, G. A. Howie, A. K. Verma, Y. Nagao, R. G. Dailey, Jr., V. A. Zimmerly, W. C. Sumner, Jr., *J. Org. Chem.* **1977**, *42*, 2349–2357.
- [6] S. Remillard, L. I. Rebhun, G. A. Howie, S. M. Kupchan, *Science* **1975**, *189*, 1002–1005.
- [7] B. F. Issell, S. T. Crooke, *Cancer Treat. Rev.* **1978**, *5*, 199–207.
- [8] G. R. Pettit, Y. Kamano, C. L. Herald, A. A. Tuinman, F. E. Boettner, H. Kizu, J. M. Schmidt, L. Baczynskyj, K. B. Tomer, R. J. Bontems, *J. Am. Chem. Soc.* **1987**, *109*, 6883–6885.
- [9] G. R. Pettit, Y. Kamano, C. Dufresne, R. L. Cerny, C. L. Herald, J. M. Schmidt, *J. Org. Chem.* **1989**, *54*, 6005–6006.
- [10] H. C. Pitot, E. A. McElroy, Jr., J. M. Reid, A. J. Windebank, J. A. Sloan, C. Erlichman, P. G. Bagniewski, D. L. Walker, J. Rubin, R. M. Goldberg, A. A. Adjei, M. M. Ames, *Clin. Cancer Res.* **1999**, *5*, 525–531.
- [11] U. Vaishampayan, M. Glode, W. Du, A. Kraft, G. Hudes, J. Wright, M. Hussain, *Clin. Cancer Res.* **2000**, *6*, 4205–4208.
- [12] R. S. Al-awar, J. E. Ray, R. M. Schultz, S. L. Andis, J. H. Kennedy, R. E. Moore, J. Liang, T. Golakoti, G. V. Subbaraju, T. H. Corbett, *J. Med. Chem.* **2003**, *46*, 2985–3007.
- [13] M. J. Edelman, D. R. Gandara, P. Hausner, V. Israel, D. Thornton, J. DeSanto, L. A. Doyle, *Lung Cancer* **2003**, *39*, 197–199.
- [14] S. Jain, L. T. Vahdat, *Clin. Cancer Res.* **2011**, *17*, 6615–6622.
- [15] M. A. Warpehoski, I. Gebhard, R. C. Kelly, W. C. Krueger, L. H. Li, J. P. McGovren, M. D. Prairie, N. Wicniewski, W. Wierenga, *J. Med. Chem.* **1988**, *31*, 590–603.
- [16] M. Cristofanilli, W. J. Bryan, L. L. Miller, A. Y. Chang, W. J. Gradishar, D. W. Kufe, G. N. Hortobagyi, *Anticancer Drugs* **1998**, *9*, 779–782.
- [17] N. Pavlidis, S. Aamdal, A. Awada, H. Calvert, P. Fumoleau, R. Sorio, C. Punt, J. Verweij, A. van Oosterom, R. Morant, J. Wanders, A. R. Hanauske, *Cancer Chemother. Pharmacol.* **2000**, *46*, 167–171.
- [18] H. C. Pitot, J. M. Reid, J. A. Sloan, M. M. Ames, A. A. Adjei, J. Rubin, P. G. Bagniewski, P. Atherton, D. Rayson, R. M. Goldberg, C. Erlichman, *Clin. Cancer Res.* **2002**, *8*, 712–717.
- [19] S. N. Markovic, V. J. Suman, A. M. Vukov, T. R. Fitch, D. W. Hillman, A. A. Adjei, S. R. Alberts, J. S. Kaur, T. A. Braich, J. M. Leitch, E. T. Creagan, *Am. J. Clin. Oncol.* **2002**, *25*, 308–312.
- [20] D. Hochhauser, T. Meyer, V. J. Spanswick, J. Wu, P. H. Clingen, P. Loadman, M. Cobb, L. Gumbrell, R. H. Begent, J. A. Hartley, D. Jodrell, *Clin. Cancer Res.* **2009**, *15*, 2140–2147.
- [21] J. Zhang, P. L. Yang, N. S. Gray, *Nat. Rev. Cancer* **2009**, *9*, 28–39.
- [22] A. Arora, E. M. Scholar, *J. Pharmacol. Exp. Ther.* **2005**, *315*, 971–979.
- [23] P. S. Low, W. A. Henne, D. D. Doorneweerd, *Acc. Chem. Res.* **2008**, *41*, 120–129.
- [24] J. A. Reddy, R. Dorton, E. Westrick, A. Dawson, T. Smith, L. C. Xu, M. Vetzel, P. Kleindl, I. R. Vlahov, C. P. Leamon, *Cancer Res.* **2007**, *67*, 4434–4442.
- [25] I. R. Vlahov, C. P. Leamon, *Bioconjugate Chem.* **2012**, *23*, 1357–1369.
- [26] G. Köhler, C. Milstein, *Nature* **1975**, *256*, 495–497.
- [27] R. K. Oldham, R. O. Dillman, *J. Clin. Oncol.* **2008**, *26*, 1774–1777.
- [28] A. M. Scott, J. D. Wolchok, L. J. Old, *Nat. Rev. Cancer* **2012**, *12*, 278–287.
- [29] L. M. Nadler, P. Stashenko, R. Hardy, W. D. Kaplan, L. N. Button, D. W. Kufe, K. H. Antman, S. F. Schlossman, *Cancer Res.* **1980**, *40*, 3147–3154.
- [30] J. C. Almagro, J. Fransson, *Front. Biosci.* **2008**, *13*, 1619–1633.
- [31] D. G. Maloney, A. J. Grillo-Lopez, C. A. White, D. Bodkin, R. J. Schilder, J. A. Neidhart, N. Janakiraman, K. A. Foon, T. M. Liles, B. K. Dallaire, K. Wey, I. Royston, T. Davis, R. Levy, *Blood* **1997**, *90*, 2188–2195.
- [32] P. Uadia, A. H. Blair, T. Ghose, *Cancer Res.* **1984**, *44*, 4263–4266.
- [33] B. C. Laguzza, C. L. Nichols, S. L. Briggs, G. J. Cullinan, D. A. Johnson, J. J. Starling, A. L. Baker, T. F. Bumol, J. R. F. Corvalan, *J. Med. Chem.* **1989**, *32*, 548–555.
- [34] P. A. Trail, D. Willner, S. J. Lasch, A. J. Henderson, S. Hofstead, A. M. Casazza, R. A. Firestone, I. Hellstrom, K. E. Hellstrom, *Science* **1993**, *261*, 212–215.
- [35] D. J. Elias, L. E. Kline, B. A. Robbins, H. C. Johnson, Jr., K. Pekny, M. Benz, J. A. Robb, L. E. Walker, M. Kosty, R. O. Dillman, *Am. J. Respir. Crit. Care Med.* **1994**, *150*, 1114–1122.
- [36] D. Schneck, F. Butler, W. Dugan, D. Littrell, B. Petersen, R. Bowsher, A. DeLong, S. Dorrbecker, *Clin. Pharmacol. Ther.* **1990**, *47*, 36–41.
- [37] B. H. Petersen, S. V. DeHerdt, D. W. Schneck, T. F. Bumol, *Cancer Res.* **1991**, *51*, 2286–2290.
- [38] A. W. Tolcher, S. Sugarman, K. A. Gelmon, R. Cohen, M. Saleh, C. Isaacs, L. Young, D. Healey, N. Onetto, W. Slichenmyer, *J. Clin. Oncol.* **1999**, *17*, 478–484.
- [39] H. H. Sedlacek, *Antibodies as Carriers of Cytotoxicity*, Karger, Basel, **1992**.
- [40] S. I. Rudnick, J. Lou, C. C. Shaller, Y. Tang, A. J. Klein-Szanto, L. M. Weiner, J. D. Marks, G. P. Adams, *Cancer Res.* **2011**, *71*, 2250–2259.
- [41] J. D. Orth, E. W. Krueger, S. G. Weller, M. A. McNiven, *Cancer Res.* **2006**, *66*, 3603–3610.
- [42] C. Dumontet, M. A. Jordan, *Nat. Rev. Drug Discovery* **2010**, *9*, 790–803.
- [43] M. Abal, J. M. Andreu, I. Barasoain, *Curr. Cancer Drug Targets* **2003**, *3*, 193–203.
- [44] K. E. Gascoigne, S. S. Taylor, *J. Cell Sci.* **2009**, *122*, 2579–2585.
- [45] J. A. Hadfield, S. Ducki, N. Hirst, A. T. McGown, *Prog. Cell Cycle Res.* **2003**, *5*, 309–325.
- [46] W. I. Lencer, R. S. Blumberg, *Trends Cell Biol.* **2005**, *15*, 5–9.
- [47] M. Lopus, E. Oroudjev, L. Wilson, S. Wilhelm, W. Widdison, R. Chari, M. A. Jordan, *Mol. Cancer Ther.* **2010**, *9*, 2689–2699.
- [48] R. H. Blum, T. Kahlert, *Cancer Treat. Rep.* **1978**, *62*, 435–438.
- [49] G. Wu, Y. Z. Fang, S. Yang, J. R. Lupton, N. D. Turner, *J. Nutr.* **2004**, *134*, 489–492.
- [50] B. J. Mills, C. A. Lang, *Biochem. Pharmacol.* **1996**, *52*, 401–406.

- [51] J. M. Cassady, K. K. Chan, H. G. Floss, E. Leistner, *Chem. Pharm. Bull.* **2004**, 52, 1–26.
- [52] C. W. Wayne, D. W. Sharon, E. C. Emily, R. W. Kathleen, A. L. Barbara, Y. Kovtun, S. G. Victor, H. Xie, M. S. Rita, J. L. Robert, R. Zhao, L. Wang, A. B. Walter, V. J. C. Ravi, *J. Med. Chem.* **2006**, 49, 4392–4408.
- [53] M. Bénéchie, F. Khuong-Huu, *J. Org. Chem.* **1996**, 61, 7133–7138.
- [54] A. I. Meyers, P. J. Reider, A. I. Campbell, *J. Am. Chem. Soc.* **1980**, 102, 6597–6598.
- [55] M. Kitamura, M. Isobe, Y. Ichikawa, T. Goto, *J. Am. Chem. Soc.* **1984**, 106, 3252–3257.
- [56] B. A. Kellogg, L. Garrett, Y. Kovtun, K. C. Lai, B. Leece, M. Miller, G. Payne, R. Steeves, K. R. Whiteman, W. Widdison, H. Xie, R. Singh, R. V. Chari, J. M. Lambert, R. J. Lutz, *Bioconjugate Chem.* **2011**, 22, 717–727.
- [57] Y. V. Kovtun, C. A. Audette, Y. Ye, H. Xie, M. F. Ruberti, S. J. Phinney, B. A. Leece, T. Chittenden, W. A. Blattler, V. S. Goldmacher, *Cancer Res.* **2006**, 66, 3214–3221.
- [58] O. Ab, L. Rui, J. Coccia, H. A. Johnson, K. R. Whiteman, B. Kellogg, L. Clancy, X. Sun, V. S. Goldmacher, *American Association for Cancer Research 102nd Annual Meeting abstract 4576, Vol. Supplement 1*, Orlando, **2011**.
- [59] E. Maloney, N. Fishkin, R. Chari, R. Singh, *Mol. Cancer Ther.* **2009**, 8, B120.
- [60] H. K. Erickson, P. U. Park, W. C. Widdison, Y. V. Kovtun, L. M. Garrett, K. Hoffman, R. J. Lutz, V. S. Goldmacher, W. A. Blattler, *Cancer Res.* **2006**, 66, 4426–4433.
- [61] M. Heine, B. Freund, P. Nielsen, C. Jung, R. Reimer, H. Hohenberg, U. Zangemeister-Wittke, H. J. Wester, G. H. Luers, U. Schumacher, *PLoS One* **2012**, 7, e36258.
- [62] Y. V. Kovtun, C. A. Audette, M. F. Mayo, G. E. Jones, H. Doherty, E. K. Maloney, H. K. Erickson, X. Sun, S. Wilhelm, O. Ab, K. C. Lai, W. C. Widdison, B. Kellogg, H. Johnson, J. Pinkas, R. J. Lutz, R. Singh, V. S. Goldmacher, R. V. Chari, *Cancer Res.* **2010**, 70, 2528–2537.
- [63] R. Zhao, S. Wilhelm, C. Audette, G. Jones, B. Leece, A. Lazar, V. Goldmacher, R. Singh, Y. Kovtun, W. Widdison, J. Lambert, R. Chari, *J. Med. Chem.* **2011**, 54, 3606–3623.
- [64] R. K. Kelly, D. L. Olson, Y. Sun, D. Wen, K. A. Wortham, G. Antognetti, A. E. Cheung, O. E. Orozco, L. Yang, V. Bailly, M. Sanicola, *Eur. J. Cancer* **2011**, 47, 1736–1746.
- [65] H. K. Erickson, G. D. L. Phillips, D. D. Leipold, C. A. Provenzano, E. Mai, H. A. Johnson, B. Gunter, C. A. Audette, M. Gupta, J. Pinkas, J. Tibbitts, *Mol. Cancer Ther.* **2012**, 11, 1133–1142.
- [66] X. Sun, W. Widdison, M. Mayo, S. Wilhelm, B. Leece, R. Chari, R. Singh, H. Erickson, *Bioconjugate Chem.* **2011**, 22, 728–735.
- [67] R. K. Pettit, G. R. Pettit, K. C. Hazen, *Antimicrob. Agents Chemother.* **1998**, 42, 2961–2965.
- [68] G. R. Pettit, J. K. Srirangam, J. Barkoczy, M. D. Williams, M. R. Boyd, E. Hamel, R. K. Pettit, F. Hogan, R. Bai, J. C. Chapuis, S. C. McAllister, J. M. Schmidt, *Anticancer Drug Des.* **1998**, 13, 243–277.
- [69] S. O. Doronina, B. A. Mendelsohn, T. D. Bovee, C. G. Cervený, S. C. Alley, D. L. Meyer, E. Oflazoglu, B. E. Toki, R. J. Sanderson, R. F. Zabinski, A. F. Wahl, P. D. Senter, *Bioconjugate Chem.* **2006**, 17, 114–124.
- [70] C. L. Law, K. A. Gordon, B. E. Toki, A. K. Yamane, M. A. Hering, C. G. Cervený, J. M. Petroziello, M. C. Ryan, L. Smith, R. Simon, G. Sauter, E. Oflazoglu, S. O. Doronina, D. L. Meyer, J. A. Francisco, P. Carter, P. D. Senter, J. A. Copland, C. G. Wood, A. F. Wahl, *Cancer Res.* **2006**, 66, 2328–2337.
- [71] S. O. Doronina, B. E. Toki, M. Y. Torgov, B. A. Mendelsohn, C. G. Cervený, D. F. Chace, R. L. DeBlanc, R. P. Gearing, T. D. Bovee, C. B. Siegall, J. A. Francisco, A. F. Wahl, D. L. Meyer, P. D. Senter, *Nat. Biotechnol.* **2003**, 21, 778–784.
- [72] S. Kaur, K. Xu, O. M. Saad, R. C. Dere, M. Carrasco-Triguero, *Bioanalysis* **2013**, 5, 201–226.
- [73] K. J. Hamblett, P. D. Senter, D. F. Chace, M. M. Sun, J. Lenox, C. G. Cervený, K. M. Kissler, S. X. Bernhardt, A. K. Kopcha, R. F. Zabinski, D. L. Meyer, J. A. Francisco, *Clin. Cancer Res.* **2004**, 10, 7063–7070.
- [74] N. M. Okeley, J. B. Miyamoto, X. Zhang, R. J. Sanderson, D. R. Benjamin, E. L. Sievers, P. D. Senter, S. C. Alley, *Clin. Cancer Res.* **2010**, 16, 888–897.
- [75] L. M. Smith, A. Nesterova, S. C. Alley, M. Y. Torgov, P. J. Carter, *Mol. Cancer Ther.* **2006**, 5, 1474–1482.
- [76] S. C. Alley, X. Zhang, N. M. Okeley, M. Anderson, C. L. Law, P. D. Senter, D. R. Benjamin, *J. Pharmacol. Exp. Ther.* **2009**, 330, 932–938.
- [77] M. D. Lee, T. S. Dunne, M. M. Siegel, C. C. Chang, G. O. Morton, D. B. Borders, *J. Am. Chem. Soc.* **1987**, 109, 3464–3466.
- [78] M. D. Lee, T. S. Dunne, C. C. Chang, G. A. Ellestad, M. M. Siegel, G. O. Morton, W. J. McGahren, D. B. Borders, *J. Am. Chem. Soc.* **1987**, 109, 3466–3468.
- [79] M. D. Lee, G. A. Ellestad, D. B. Borders, *Acc. Chem. Res.* **1991**, 24, 235–243.
- [80] A. L. Smith, K. C. Nicolaou, *J. Med. Chem.* **1996**, 39, 2103–2117.
- [81] K. C. Nicolaou, C. R. H. Hale, C. Nilewski, *Chem. Rec.* **2012**, 12, 407–441.
- [82] N. Zein, A. M. Sinha, W. J. McGahren, G. A. Ellestad, *Science* **1988**, 240, 1198–1201.
- [83] R. G. Bergman, *Acc. Chem. Res.* **1973**, 6, 25–31.
- [84] L. M. Hinman, P. R. Hamann, R. Wallace, A. T. Menendez, F. E. Durr, J. Upeslaci, *Cancer Res.* **1993**, 53, 3336–3342.
- [85] P. R. Hamann, L. M. Hinman, C. F. Beyer, D. Lindh, J. Upeslaci, D. A. Flowers, I. Bernstein, *Bioconjugate Chem.* **2002**, 13, 40–46.
- [86] P. R. Hamann, L. M. Hinman, C. F. Beyer, L. M. Greenberger, C. Lin, D. Lindh, A. T. Menendez, R. Wallace, F. E. Durr, J. Upeslaci, *Bioconjugate Chem.* **2005**, 16, 346–353.
- [87] P. R. Hamann, L. M. Hinman, C. F. Beyer, D. Lindh, J. Upeslaci, D. Shochat, A. Mountain, *Bioconjugate Chem.* **2005**, 16, 354–360.
- [88] P. R. Hamann, L. M. Hinman, I. Hollander, C. F. Beyer, D. Lindh, R. Holcomb, W. Hallett, H. R. Tsou, J. Upeslaci, D. Shochat, A. Mountain, D. A. Flowers, I. Bernstein, *Bioconjugate Chem.* **2002**, 13, 47–58.
- [89] J. F. DiJoseph, M. M. Dougher, D. Y. Evans, B. B. Zhou, N. K. Damle, *Cancer Chemother. Pharmacol.* **2011**, 67, 741–749.
- [90] F. Kratz, P. Senter, H. Steinhagen, *Drug Delivery in Oncology: From Basic Research to Cancer Therapy*, Wiley-VCH, Weinheim, **2012**.
- [91] A. Advani, B. Coiffier, M. S. Czuczman, M. Dreyling, J. Foran, E. Gine, C. Gisselbrecht, N. Ketterer, S. Nasta, A. Rohatiner, I. G. Schmidt-Wolf, M. Schuler, J. Sierra, M. R. Smith, G. Verhoef, J. N. Winter, J. Boni, E. Vandendries, M. Shapiro, L. Fayad, *J. Clin. Oncol.* **2010**, 28, 2085–2093.
- [92] M. Ichimura, T. Ogawa, S. Katsumata, K. Takahashi, I. Takahashi, H. Nakano, *J. Antibiot.* **1991**, 44, 1045–1053.
- [93] L. J. Hanka, A. Dietz, S. A. Gerpheide, S. L. Kuentzel, D. G. Martin, *J. Antibiot.* **1978**, 31, 1211–1217.
- [94] B. K. Bhuyan, K. A. Newell, S. L. Crampton, D. D. Von Hoff, *Cancer Res.* **1982**, 42, 3532–3537.
- [95] D. L. Boger, D. S. Johnson, *Proc. Natl. Acad. Sci. USA* **1995**, 92, 3642–3649.
- [96] L. H. Li, T. F. DeKoning, R. C. Kelly, W. C. Krueger, J. P. McGovern, G. E. Padbury, G. L. Petzold, T. L. Wallace, R. J. Ouding, M. D. Prairie, I. Gebhard, *Cancer Res.* **1992**, 52, 4904–4913.

- [97] C. S. Lee, G. P. Pfeifer, N. W. Gibson, *Biochemistry* **1994**, *33*, 6024–6030.
- [98] R. Baird, S. Winstein, *J. Am. Chem. Soc.* **1957**, *79*, 4238–4240.
- [99] D. L. Boger, C. W. Boyce, R. M. Garbaccio, J. A. Goldberg, *Chem. Rev.* **1997**, *97*, 787–828.
- [100] D. L. Boger, W. Yun, B. R. Teegarden, *J. Org. Chem.* **1992**, *57*, 2873–2876.
- [101] D. L. Boger, J. A. McKie, *J. Org. Chem.* **1995**, *60*, 1271–1275.
- [102] R. V. Chari, K. A. Jackel, L. A. Bourret, S. M. Derr, B. M. Tadayoni, K. M. Mattocks, S. A. Shah, C. Liu, W. A. Blattler, V. S. Goldmacher, *Cancer Res.* **1995**, *55*, 4079–4084.
- [103] R. Y. Zhao, H. K. Erickson, B. A. Leece, E. E. Reid, V. S. Goldmacher, J. M. Lambert, R. V. Chari, *J. Med. Chem.* **2012**, *55*, 766–782.
- [104] W. Dokter, P. Beusker, G. Verheijden, R. Ubink, M. v. d. Lee, D. v. d. Dobbelssteen, P. Goedings, J. Lemmens, V. d. Groot, M. Timmers, *AACR National Meeting (Washington, D. C.)* **2013**, Abstr. 4329.
- [105] M. E. Wall, M. C. Wani, C. E. Cook, K. H. Palmer, A. T. McPhail, G. A. Sim, *J. Am. Chem. Soc.* **1966**, *88*, 3888–3890.
- [106] Y. H. Hsiang, R. Hertzberg, S. Hecht, L. F. Liu, *J. Biol. Chem.* **1985**, *260*, 14873–14878.
- [107] R. H. Mathijssen, R. J. van Alphen, J. Verweij, W. J. Loos, K. Nooter, G. Stoter, A. Sparreboom, *Clin. Cancer Res.* **2001**, *7*, 2182–2194.
- [108] W. D. Kingsbury, J. C. Boehm, D. R. Jakas, K. G. Holden, S. M. Hecht, G. Gallagher, M. J. Caranfa, F. L. McCabe, L. F. Faucette, R. K. Johnson, R. P. Hertzberg, *J. Med. Chem.* **1991**, *34*, 98–107.
- [109] S. J. Moon, S. V. Govindan, T. M. Cardillo, C. A. D'Souza, H. J. Hansen, D. M. Goldenberg, *J. Med. Chem.* **2008**, *51*, 6916–6926.
- [110] R. M. Sharkey, S. V. Govindan, T. M. Cardillo, D. M. Goldenberg, *Mol. Cancer Ther.* **2012**, *11*, 224–234.
- [111] R. Stein, M. J. Mattes, T. M. Cardillo, H. J. Hansen, C. H. Chang, J. Burton, S. Govindan, D. M. Goldenberg, *Clin. Cancer Res.* **2007**, *13*, 5556s–5563s.
- [112] S. V. Govindan, T. M. Cardillo, R. M. Sharkey, F. Tat, D. V. Gold, D. M. Goldenberg, *Mol. Cancer Ther.* **2013**, *12*, 968–978.
- [113] S. V. Govindan, T. M. Cardillo, S. J. Moon, H. J. Hansen, D. M. Goldenberg, *Clin. Cancer Res.* **2009**, *15*, 6052–6061.
- [114] T. M. Cardillo, S. V. Govindan, R. M. Sharkey, P. Trisal, D. M. Goldenberg, *Clin. Cancer Res.* **2011**, *17*, 3157–3169.
- [115] P. F. Bross, J. Beitz, G. Chen, X. H. Chen, E. Duffy, L. Kieffer, S. Roy, R. Sridhara, A. Rahman, G. Williams, R. Pazdur, *Clin. Cancer Res.* **2001**, *7*, 1490–1496.
- [116] S. H. Petersdorf, K. J. Kopecky, M. Slovak, C. Willman, T. Nevill, J. Brandwein, R. A. Larson, H. P. Erba, P. J. Stiff, R. K. Stuart, R. B. Walter, M. S. Tallman, L. Stenke, F. R. Appelbaum, *Blood* **2013**, *121*, 4854–4860.
- [117] J. M. Rowe, B. Lowenberg, *Blood* **2013**, *121*, 4838–4841.
- [118] M. S. Sutherland, R. J. Sanderson, K. A. Gordon, J. Andreyka, C. G. Cerveney, C. Yu, T. S. Lewis, D. L. Meyer, R. F. Zabinski, S. O. Doronina, P. D. Senter, C. L. Law, A. F. Wahl, *J. Biol. Chem.* **2006**, *281*, 10540–10547.
- [119] S. M. Ansell, S. M. Horwitz, A. Engert, K. D. Khan, T. Lin, R. Strair, T. Keler, R. Graziano, D. Blanset, M. Yellin, S. Fischkoff, A. Assad, P. Borchmann, *J. Clin. Oncol.* **2007**, *25*, 2764–2769.
- [120] J. Katz, J. E. Janik, A. Younes, *Clin. Cancer Res.* **2011**, *17*, 6428–6436.
- [121] A. Younes, A. K. Gopal, S. E. Smith, S. M. Ansell, J. D. Rosenblatt, K. J. Savage, R. Ramchandren, N. L. Bartlett, B. D. Cheson, S. de Vos, A. Forero-Torres, C. H. Moskowitz, J. M. Connors, A. Engert, E. K. Larsen, D. A. Kennedy, E. L. Sievers, R. Chen, *J. Clin. Oncol.* **2012**, *30*, 2183–2189.
- [122] A. Younes, N. L. Bartlett, J. P. Leonard, D. A. Kennedy, C. M. Lynch, E. L. Sievers, A. Forero-Torres, *N. Engl. J. Med.* **2010**, *363*, 1812–1821.
- [123] S. Verma, D. Miles, L. Gianni, I. E. Krop, M. Welslau, J. Baselga, M. Pegram, D. Y. Oh, V. Dieras, E. Guardino, L. Fang, M. W. Lu, S. Olsen, K. Blackwell, *N. Engl. J. Med.* **2012**, *367*, 1783–1791.
- [124] H. A. Burris III, H. S. Rugo, S. J. Vukelja, C. L. Vogel, R. A. Borson, S. Limentani, E. Tan-Chiu, I. E. Krop, R. A. Michaelson, S. Girish, L. Amler, M. Zheng, Y. W. Chu, B. Klencke, J. A. O'Shaughnessy, *J. Clin. Oncol.* **2011**, *29*, 398–405.
- [125] S. A. Hurvitz, L. Dirix, J. Kocsis, G. V. Bianchi, J. Lu, J. Vinholes, E. Guardino, C. Song, B. Tong, V. Ng, Y. W. Chu, E. A. Perez, *J. Clin. Oncol.* **2013**, *31*, 1157–1163.
- [126] H. Kantarjian, D. Thomas, J. Jorgensen, E. Jabbour, P. Kebriaei, M. Rytting, S. York, F. Ravandi, M. Kwari, S. Faderl, M. B. Rios, J. Cortes, L. Fayad, R. Tarnai, S. A. Wang, R. Champlin, A. Advani, S. O'Brien, *Lancet Oncol.* **2012**, *13*, 403–411.
- [127] W. Leimgruber, A. D. Batcho, F. Schenker, *J. Am. Chem. Soc.* **1965**, *87*, 5793–5795.
- [128] W. Leimgruber, V. Stefanovic, F. Schenker, A. Karr, J. Berger, *J. Am. Chem. Soc.* **1965**, *87*, 5791–5793.
- [129] D. Antonow, D. E. Thurston, *Chem. Rev.* **2011**, *111*, 2815–2864.
- [130] D. S. Bose, A. S. Thompson, J. Ching, J. A. Hartley, M. D. Berardini, T. C. Jenkins, S. Neidle, L. H. Hurley, D. E. Thurston, *J. Am. Chem. Soc.* **1992**, *114*, 4939–4941.
- [131] S. J. Gregson, P. W. Howard, J. A. Hartley, N. A. Brooks, L. J. Adams, T. C. Jenkins, L. R. Kelland, D. E. Thurston, *J. Med. Chem.* **2001**, *44*, 737–748.
- [132] J. A. Hartley, V. J. Spanswick, N. Brooks, P. H. Clingen, P. J. McHugh, D. Hochhauser, R. B. Pedley, L. R. Kelland, M. C. Alley, R. Schultz, M. G. Hollingshead, K. M. Schweikart, J. E. Tomaszewski, E. A. Sausville, S. J. Gregson, P. W. Howard, D. E. Thurston, *Cancer Res.* **2004**, *64*, 6693–6699.
- [133] M. C. Alley, M. G. Hollingshead, C. M. Pacula-Cox, W. R. Waud, J. A. Hartley, P. W. Howard, S. J. Gregson, D. E. Thurston, E. A. Sausville, *Cancer Res.* **2004**, *64*, 6700–6706.
- [134] J. A. Hartley, A. Hamaguchi, M. Coffils, C. R. Martin, M. Suggitt, Z. Chen, S. J. Gregson, L. A. Masterson, A. C. Tiberghien, J. M. Hartley, C. Pepper, T. T. Lin, C. Fegan, D. E. Thurston, P. W. Howard, *Cancer Res.* **2010**, *70*, 6849–6858.
- [135] M. Miller, N. Fishkin, W. Li, B. Leece, M. Mayo, G. Jones, E. Reid, K. Archer, E. Maloney, Y. Kovtun, J. Pinkas, R. Singh, R. Chari, *Mol. Cancer Ther.* **2009**, *8*, B126.
- [136] S. C. Jeffrey, P. J. Burke, R. P. Lyon, D. W. Meyer, D. Sussman, M. Anderson, J. H. Hunter, C. I. Leiske, J. B. Miyamoto, N. D. Nicholas, N. M. Okeley, R. J. Sanderson, I. J. Stone, W. Zeng, S. J. Gregson, L. Masterson, A. C. Tiberghien, P. W. Howard, D. E. Thurston, C. L. Law, P. D. Senter, *Bioconjugate Chem.* **2013**, *24*, 1256–1263.
- [137] M. S. Kung Sutherland, R. B. Walter, S. C. Jeffrey, P. J. Burke, C. Yu, H. Kostner, I. Stone, M. C. Ryan, D. Sussman, R. P. Lyon, W. Zeng, K. H. Harrington, K. Klussman, L. Westendorf, D. Meyer, I. D. Bernstein, P. D. Senter, D. R. Benjamin, J. G. Drachman, J. A. McEarchern, *Blood* **2013**, *122*, 1455–1463.
- [138] J. Anderl, C. Muller, B. Heckl-Ostreicher, R. Wehr, *Cancer Res.* **2011**, *71*, 3616.
- [139] A. C. Lazar, L. Wang, W. A. Blattler, G. Amphlett, J. M. Lambert, W. Zhang, *Rapid Commun. Mass Spectrom.* **2005**, *19*, 1806–1814.
- [140] A. Wakankar, Y. Chen, Y. Gokarn, F. S. Jacobson, *MABS* **2011**, *3*, 161–172.
- [141] J. R. Junutula, H. Raab, S. Clark, S. Bhakta, D. D. Leipold, S. Weir, Y. Chen, M. Simpson, S. P. Tsai, M. S. Dennis, Y. Lu, Y. G. Meng, C. Ng, J. Yang, C. C. Lee, E. Duenas, J. Gorrell, V. Katta, A. Kim, K. McDorman, K. Flagella, R. Venook, S. Ross, S. D. Spencer, W. L. Wong, H. B. Lowman, R. Vandlen, M. X.

- Sliwkowski, R. H. Scheller, P. Polakis, W. Mallet, *Nat. Biotechnol.* **2008**, *26*, 925–932.
- [142] A. Yurkovetskiy, N. Bodyak, M. Yin, J. Thomas, P. Conlon, C. Stevenson, A. Uttard, L. Qin, A. Campbell, D. Gumerov, E. Ter-Ovanesyan, M. DeVit, T. Lowinger, in *AACR National Meeting (Washington, D. C.) 2013*, Abstr. 4331.
- [143] J. B. Stimmel, B. M. Merrill, L. F. Kuyper, C. P. Moxham, J. T. Hutchins, M. E. Fling, F. C. Kull, Jr., *J. Biol. Chem.* **2000**, *275*, 30445–30450.
- [144] B. Q. Shen, K. Xu, L. Liu, H. Raab, S. Bhakta, M. Kenrick, K. L. Parsons-Reponte, J. Tien, S. F. Yu, E. Mai, D. Li, J. Tibbitts, J. Baudys, O. M. Saad, S. J. Scales, P. J. McDonald, P. E. Hass, C. Eigenbrot, T. Nguyen, W. A. Solis, R. N. Fuji, K. M. Flagella, D. Patel, S. D. Spencer, L. A. Khawli, A. Ebens, W. L. Wong, R. Vandlen, S. Kaur, M. X. Sliwkowski, R. H. Scheller, P. Polakis, J. R. Junutula, *Nat. Biotechnol.* **2012**, *30*, 184–189.
- [145] J. Y. Axup, K. M. Bajjuri, M. Ritland, B. M. Hutchins, C. H. Kim, S. A. Kazane, R. Halder, J. S. Forsyth, A. F. Santidrian, K. Stafin, Y. Lu, H. Tran, A. J. Seller, S. L. Biroc, A. Szydluk, J. K. Pinkstaff, F. Tian, S. C. Sinha, B. Felding-Habermann, V. V. Smider, P. G. Schultz, *Proc. Natl. Acad. Sci. USA* **2012**, *109*, 16101–16106.
- [146] P. Strop, S. H. Liu, M. Dorywalska, K. Delaria, R. G. Dushin, T. T. Tran, W. H. Ho, S. Farias, M. G. Casas, Y. Abdiche, D. Zhou, R. Chandrasekaran, C. Samain, C. Loo, A. Rossi, M. Rickert, S. Krimm, T. Wong, S. M. Chin, J. Yu, J. Dilley, J. Chaparro-Riggers, G. F. Filzen, C. J. O'Donnell, F. Wang, J. S. Myers, J. Pons, D. L. Shelton, A. Rajpal, *Chem. Biol.* **2013**, *20*, 161–167.
- [147] S. Möhlmann, P. Bringmann, S. Greven, A. Harrenga, *BMC Biotechnol.* **2011**, *11*, 76.
- [148] G. Casi, N. Huguenin-Dezot, K. Zuberbühler, J. Scheuermann, D. Neri, *J. Am. Chem. Soc.* **2012**, *134*, 5887–5892.
- [149] T. Yokota, D. E. Milenic, M. Whitlow, J. Schlom, *Cancer Res.* **1992**, *52*, 3402–3408.
- [150] K. M. Kim, C. F. McDonagh, L. Westendorf, L. L. Brown, D. Sussman, T. Feist, R. Lyon, S. C. Alley, N. M. Okeley, X. Zhang, M. C. Thompson, I. Stone, H. P. Gerber, P. J. Carter, *Mol. Cancer Ther.* **2008**, *7*, 2486–2497.
- [151] G. J. Bernardes, G. Casi, S. Trussel, I. Hartmann, K. Schwager, J. Scheuermann, D. Neri, *Angew. Chem.* **2012**, *124*, 965–968; *Angew. Chem. Int. Ed.* **2012**, *51*, 941–944.